Performance Evaluation of CBN Tools in High-Speed Dry Turning of AISI 1018 Low Carbon Steel

Performance Evaluation of CBN Tools in High-Speed Dry Turning of AISI 1018 Low Carbon Steel

BY
Kan Zhang, B. Eng.

A Thesis
Submitted to the School of Graduate Studies
in Partial Fulfillment of the Requirements
for the Degree
Master of Applied Science

McMaster University

Hamilton, Ontario, Canada

Master of Applied Science (2019) McMaster University

(Mechanical Engineering) Hamilton, Ontario, Canada

TITLE: PERFORMANCE EVALUATION OF CBN TOOLS IN HIGH-SPEED DRY TURNING OF AISI 1018 LOW CARBON STEEL

AUTHOR: Kan Zhang B. Eng., Mechanical Engineering

SUPERVISOR: Dr. Stephen C. Veldhuis

Department of Mechanical Engineering

McMaster University

NUMBER OF PAGES: xvi, 97

ABSTRACT

Increasing productivity is a constant demand for the manufacturing industry. Low-carbon-steel is one of the most commonly used ferrous materials in the part manufacturing market. Improving productivity as well as making the process eco-friendly by implementing a dry machining condition is the essential goal of this study.

Built-up-edge (BUE) is often formed in the low-carbon-steel machining process, which, results in poor surface finish and short tool life. The high-speed-machining technique can be used to reduce the BUE formation and realize an increase in productivity. Cubic boron nitride (CBN) tools are most commonly used in hard turning and cast-iron machining at high cutting speeds. There are a limited number of studies regarding low-carbon-steel machining with CBN under a high-speed and with a dry machining condition. In this study, the investigation shows the preferable type of CBN tool and the wear mechanisms involved during finish turning operations of AISI 1018 under high speed and dry machining conditions.

Test results show that a low CBN content with a TiCN binder and smaller grain size offers the best tool life and surface integrity of the final part. Currently manufacturers use coated carbide tools with a recommended cutting speed of 200-300m/min with coolant to complete the finishing process for turning low carbon steel parts. In this study, by implementing CBN tools under the dry condition at 500 m/min cutting speed (speed was selected from the preliminary test performed using the uncoated CBN from 500 to 1200 m/min), the buildup edge formation has been reduced, tool life was measured to increase by 307% compared to the benchmark tool (Coated Carbide), and surface finish was measured in the range of 0.8-1.6μm Ra.

ACKNOWLEDGEMENT

The authors would like to gratefully acknowledge the financial support received from the Natural Sciences and Engineering Research Council of Canada (NSERC) and Canadian Network for Research and Innovation in Machining Technology (CANRIMT).

I would like to thank everyone who helped me build and accomplish this thesis.

First and foremost, I want to express my deep gratitude to my supervisor Dr. S. C. Veldhuis who offered me this opportunity to continue my study in the field of mechanical and manufacturing. Your work to bring us together at McMaster Research Manufacturing Institute (MMRI). The friendly environment, easy access to support and helpful teammates are what you have created for me and every student who has studied in MMRI.

Many thanks to all the members in the research team and all the technical support provided by you particularly Terry, Brady, Simon, Jennifer, Ahmad, Dr. Arif, Dr. Jose, Dr. Fox at MMRI. Thanks for being a beacon that directs my walk out the mist of confusion during my research.

Also, I want to express my thanks to all my colleagues and friends from McMaster Manufacturing Research Institute (MMRI) for being such a great team and for making our laboratory such a pleasant place in which to work. Thanks to all the student friends I made at the MMRI group: Abdo, Khalid, Majid, Sharif, Pietro, Ednie, Rohan, Alam, Baoqin, Wanting, Qianxi, and Yesong. Special thanks to Changcheng who introduced me to MMRI and helped me walk through the valley,

made me fear no more. And thanks for Wanting for you are with me and comfort me through the last two years of my student life at McMaster.

Last and most importantly, I want to thank my mother, father, grandparents and all family members. I thank them for their constant love and care for all my life. Though they are far at home, is the bloodline which tied me with them and without their support, I would have never reached this far.

感谢父亲对我的栽培，家庭的和谐永远是最重要的。

感谢母亲对我的关爱，爱有时要比成长更令人欣喜。

感谢我的每一位亲人，在我最需要时给予我的关心与疼爱。

感谢我的每一位朋友，在我最为难时给予我的支持与鼓励。

在加拿大的这些年，感谢有你们，才有现在的张戡，至于未来的我请你们拭目以待。

I love you all. I am loving you all.

NOTATION and ABBREVIATIONS

LCS	Low-carbon Steel
HSM	High-speed machining
HSDM	High-speed dry machining
CBN	Cubic Boron Nitride
DOC	Depth of cut
f	Feed rate
v	Cutting speed
r	Cutting edge radius
yb	Negative bevel angle
by	T-land length
Ra	The arithmetic average roughness
FEA	Finite element analysis
SEM	Scanning electron microscopy
XRD	X-ray diffraction
EDS	Energy-dispersive X-ray spectrometry
PVD	Physical vapour deposition
CVD	Chemical vapour deposition
PSDZ	Primary shear deformation zone
SSDZ	Secondary shear deformation zone
TSDZ	Tertiary shear deformation zone

CONTENTS

LIST OF FIGURES

LIST OF TABLES

1 INTRODUCTION

1.1 Background

Low carbon steel (iron-containing steel with a small percentage of carbon), also known as mild steel is a type of plain-carbon steel. Due to its relatively low cost, ease of machining and material properties, it is one of the most commonly used steels. The range of carbon content in low carbon steel is between 0.05% to 0.25%, making it malleable and ductile. The material has a relatively low tensile strength and is easy to form [1]. Its surface hardness can be improved by surface treatments such as carburizing and boriding [2]. Most high-tensile steels contain low carbon as well and have additional alloying ingredients that increase their tensile strength and wear properties. These alloying ingredients include chromium, silicon, manganese, nickel, etc.

High-speed machining (HSM) was introduced in the 1990's. The main goal of applying HSM to part production is to improve the machining productivity, surface integrity and machining accuracy of suitable materials [3].

Traditionally coolant is applied at a rate of 10 – 100L/min. Coolant is used to reduce the friction and temperature in the contact area between the tool and chip, thereby increasing tool life. Coolant recirculates in the system but must be disposed of typically on a yearly basis, which generates a significant environmental burden. Most types of cutting fluid used in manufacturing may start out as environment-friendly but over time they accumulate hazardous elements and support bacteria growth. Eliminating or greatly reducing the use of coolant is far more preferable from an ecological point of view. Dry machining in conjunction with a high cutting speed can lead to a very high

temperature at the tool-chip interface, which increases the rate of tool wear during cutting [4]. Eliminating coolant use can be highly beneficial in reducing the ecological footprint of low-carbon steel machining but then the temperature factor must still be taken into account.

Cubic Boron Nitride (CBN) tools are usually used for machining applications involving difficult-to-cut materials, such as hardened steels, hard materials and cast iron. Other characteristics of CBN include abrasion, thermal and chemical resistance as well as its ability to maintain a sharp edge during cutting. CBN has also been shown to be a good option for machining ferrous materials [5].

This study strives to improve productivity without sacrificing the tool life while performing high-speed dry machining with CBN tools.

1.2 Motivation

Since mild steel is soft and sticky, it generally experiences a relatively low cutting force during the machining process but will usually have more built-up edge (BUE) formation during continuous cutting. A good edge geometry can decrease the tendency of smearing and prevent edge deterioration. BUE formation alters the geometry of the cutting edge, negatively affecting the surface quality of the machined part, the tool life and the productivity of the manufacturing process. A higher cutting speed can prevent or reduce BUE formation.

This thesis is motivated by the demand for highly productive and sustainable manufacturing processes. High-speed dry machining (HSDM) can significantly reduce the machining cycle time, thereby increasing productivity and part quality. Dry machining eliminates the need for coolant, which can reduce the manufacturing cost by 17% [6]and benefit the environment. High hardness CBN tools can endure greater loads, which makes them more wear-resistant under high cutting

speed conditions. CBN tools are thus commonly used to machine GCI, Titanium and Aluminum alloys at a high speed. Liu reported that dry machined cast iron using uncoated CBN tools, at a suitable cutting speed, can form tribofilms that act as a protective layer [7] for the machine tool, making high-speed dry machining perform better than the traditional machining method. Thus, CBN is selected for this thesis project as the basis for High-speed dry machining (HSDM) for low carbon steel (LCS).

1.3 Research Objectives

The current industry standards for machining low carbon steel (LCS) do not include high-speed dry machining, and CBN tools are rarely used.

Based on past research performed by others my main objectives for this research are:

1. Develop and apply a procedure for selecting an uncoated CBN tool for high-speed dry machining of low carbon steel through comparative studies.
2. Investigate the effect of cutting speed on tool performance for the high-speed dry machining using uncoated CBN.
3. Investigate the role of coating in improving tool life and surface integrity of machined surfaces under optimized cutting conditions.

1.4 Thesis outline

This thesis is arranged into five chapters. A brief summary of each chapter follows:

CHAPTER 1: Introduction – Outline of the motivation and the research objectives of this thesis.

CHAPTER 2: Literature review – An overview of LCS (low carbon steel), high-speed machining, dry machining, and the benefits of using carbide and CBN cutting tools.

CHAPTER 3: Methodology and Experimental Outline – Description of the experimental procedures, workpiece material properties, tool selection details, machine set-ups and parameters used in this thesis.

CHAPTER 4: Tool Characterisation – The results of tests carried out to validate the tool geometry and material properties of the selected machine inserts.

CHAPTER 5: Results and Discussion – Experimental results are provided with detailed analysis. This chapter is divided into four subsections to provide an overview of the relationship between the machine tools and the workpiece.

CHAPTER 6: Conclusion and Future Work – Recommendations for future directions of this research.

2 Literature Review

2.1 Machining

In metal cutting, machining refers to various controlled metal removal processes that remove excess material from the targeted part in the form of chips to achieve a desired geometry. The three principal machining processes are turning, milling and drilling [8]. The cutting action is achieved by means of relative motion between the tool and the workpiece. Figure 2.1 shows a cross-sectional view of the machining process.

In this research, the turning process was used for the machining tests. Turning is the machining operation in which a single point cutting tool removes excess material from a rotating workpiece to form a cylindrical shape. The cutting condition can be referred to as a continuous cut.

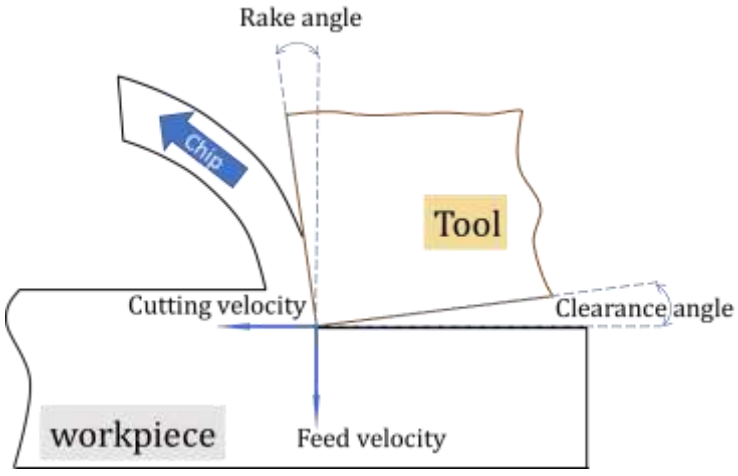

Figure 2.1 Cross-section view of the machining process [based on [8]]

2.2 Mild Steel (Work Piece Material)

AISI 1018 mild steel is one of the most commonly used low-carbon steels in the automobile, airplane, utility, medical industries, pipeline construction, building structures, railway parts, electronic devices and many others. For example, AISI 1018 is found in axles, bolts, shafts, machinery parts, gears, pinions, worms, kingpins and ratchets. Cold forming can also be applied to the material for crimping, bending or swaging. The composition of the workpiece AISI 1018 is: C- 0.18, Si - 0.15, Mn - 0.80, P - 0.018; and S - 0.027%. The material properties are: hardness - 145 HV, Toughness - 8.4 kg-m. Low carbon steel consists of mostly ferrite (65%) and pearlite (35%). Rao and Venkatasubbaiah reported that ferrite is a soft structure and pearlite is a very fine plate-like or lamellar mixture composed of ferrite and cementite [9]. Figure 2.2 below shows the microstructure of AISI 1018 mild steel. The bright area in the image is the free ferrite structure and the dark area is the pearlite structure [10].

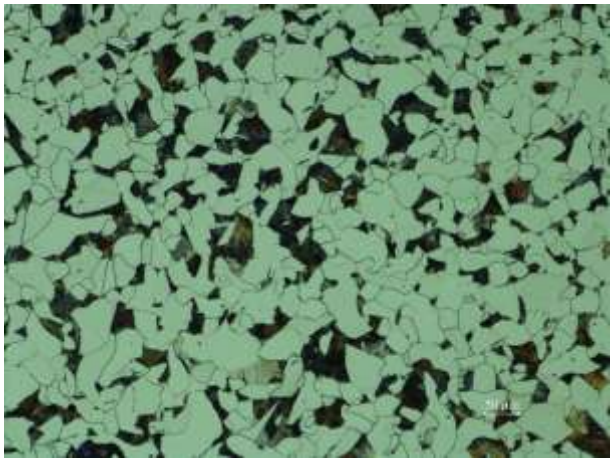

Figure 2.2 Microstructure of AISI 1018 steel at 20x, 5% Nital Etch

Chinchanikar and Choudhury report that mild steel is soft and gummy due to its low hardness which promotes adhesive wear when machining, causing chip control problems [11]. Mild steel contains mostly iron (98.81-99.26%), carbon (0.05-0.26%) and small amounts of other elements (Manganese, Mn 0.6-0.9%; Phosphorus, P 0.04% Max; Sulfur, S 0.05% Max) [9]. It comes in a variety of shapes ranging from flat sheet steel and steel bars to big steel blocks and construction beams. Due to the low carbon content, boriding and carbonizing are very common case hardening processes applied to low carbon steel to reduce mechanical wear and enhance the mechanical properties [2]. Dogra et al. reported that low carbon steel is known for its low heat treatability, due to having smaller effective hardening diameters compared to higher carbon-containing ferrous steel. Grange reported on the hardenability of carbon steels, noting that low carbon content makes hardening by quenching more difficult to perform on low carbon steels [12]. The result is that hard turning which is commonly used in place of grinding will be a less effective process for low carbon steel machining. Based on the work of Selcuk et al. and the Kennametal tool manufacturer catalogue, it can be concluded that although low-carbon steel is soft and its chips are difficult to manage, HSM is nonetheless possible due to its easy-to-machine nature [11]. According to the review paper done by Goindi and Sarkar [6], during dry machining process, low carbon ferrous alloys from the workpiece were likely to adhere to both the cutting-tool edge and rake face, which results in the formation of built-up edge (BUE). BUE is undesirable in machining because it degrades the final part's surface integrity, and causes higher cutting forces, excessive tool damage, increased friction and causes further temperature build up [13]. According to Goindi and Sarkar, HSM in conjunction with dry machining should be used to avoid thermal shock in order to prevent poor surface finish of the workpiece and cracks and fracture of the cutting tools [6]. Dry machining

at a high cutting speed leads to high temperature in the cutting zone, which accelerates the tool wear rate during cutting [4].

2.3 High-speed machining and Dry machining

2.3.1 High-speed machining

Based on the tooling catalogues [14][15][16], the recommended speed for cutting low carbon steel with a CBN tool is in the range of 120 to 420 m/min. The recommended surface speed for cutting hardened steel with CBN is 200-300 m/min. The recommended surface speed for cutting GCI with CBN is 250-800 m/min [7] [17].

Sreejith and Ngoi reported that the high-speed range for steel is 500-1200 m/min. Both carbide and CBN can be used under severe cutting conditions, but CBN can retain its hardness at a higher temperature range [18].

The main objective of HSM is to replace grinding as a finishing process for achieving good surface quality, machining accuracy and overall productivity [19]. HSM has been introduced for materials such as cast iron and aluminum alloys [17][20]. HSM can significantly affect the tool life of modern machine tools used by most manufacturers. Carbide tools have a limited maximum cutting speed where significant wear may occur. A higher cutting speed will generate a higher temperature in the cutting zone, thus drastically reducing the tool life of the carbide tool. Figure 2.3 below shows that different materials have different cutting speed ranges defined as HSM range.

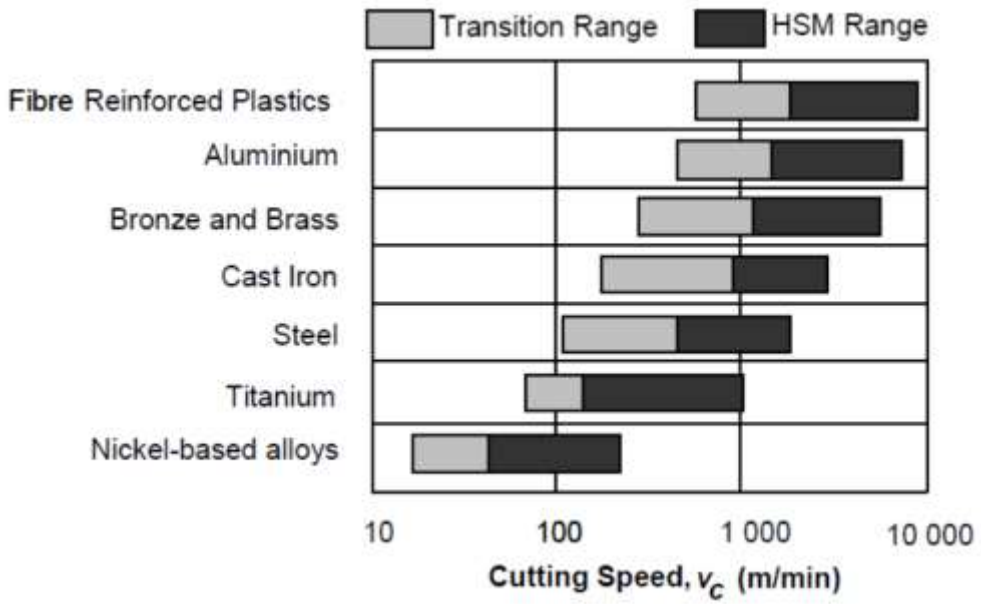

Figure 2.3 High-speed cutting ranges in machining of various materials based on [7]

In alloy steels, HSM technology is usually applied at a hardened state (Usually hardness > 30 HRC). Studies show that HSM of material at their hardened state could replace the slow EDM processes for many applications, but the HSM of hardened steels will generate high temperatures and stresses in the workpiece-tool interface [18].

2.3.2 Dry machining

HSM was introduced in 1982. Schulz and Moriwaki reported that the definition of high-cutting speed varies with different target workpiece materials and is evolving over time [3]. Mild steel machining uses a large amount of coolant, since the surface finish and tool life is sensitive to the tool-chip interference temperature. The recommended cutting fluids for the free-machining of low-carbon steels during a turning operation are general-purpose, soluble oils and semi-synthetic or

synthetic fluids [4][8]. Understanding the wear mechanisms of the cutting tool engaged in high-speed dry machining is essential for its successful implementation. The cutting speed used to machine low carbon steel is around 200 m/min for roughing and 400 m/min [21] for finishing the process under wet cutting conditions. Sreejith and Ngoi reported the performance of a cutting tool during dry machining depends on the stability of the cutting wedge, which is mostly dependent on the thermal conductivity of the work materials and the tools used [18].

Dry machining is difficult due to high temperature and short tool life. Studies should be focused on wear patterns and mechanisms, cutting forces, and the cutting zone temperature. The graph indicated that CBN and diamond tools can maintain their hardness at a higher temperature compared to carbide and High-speed steel tools. The graph below indicates that CBN tools are more suitable for higher cutting speeds, since they can retain higher hardness at a higher temperature [6]. Dogra et al. reported that the high hot hardness can benefit the chip interface temperature and improve the tool life during cutting [19].

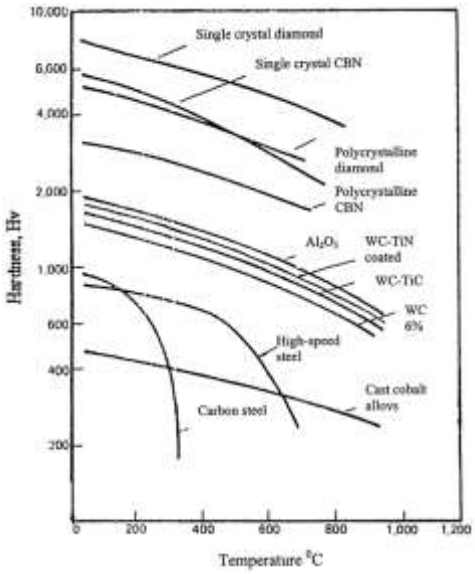

Figure 2.4 Typical hot-hardness characteristics of some tool materials [18]

2.4 Cutting tools

2.4.1 Cutting tool terminology

Turning inserts come in a variety of shapes and sizes. It is important to note that every turning insert has a nomenclature associated with it. In this cutting test the tool holder used introduced a 5-degree clearance angle during the turning process. This nomenclature provides general information about the turning inserts. Note that this is an ISO standard format for tooling.

C	N	M	G	12	04	08
1	2	3	4	5	6	7

Figure 2.5 General Turning Insert Nomenclature Over All Representation [22]

The turning insert nomenclature CNMG 120408 is the major guide of tool selection made in this thesis work. Due to the availability of CBN inserts, when the target nomenclature CNMG is unavailable the insert selection will be made from similar grade: CNMA and CNGA. The last three numbers are selected to be 120408 or 120412 (see 3.3.2 Tool Selection).

The first letter in the turning insert nomenclature refers to the general turning insert shape, as shown in the image below. The second letter refers to the insert clearance angle as referenced in figure 2.6 (b). The third letter refers to the insert's tolerance class, such as turning insert length, height etc. The fourth letter refers to the turning insert hole shape and chip breaker type as shown in figure 2.6 (c).

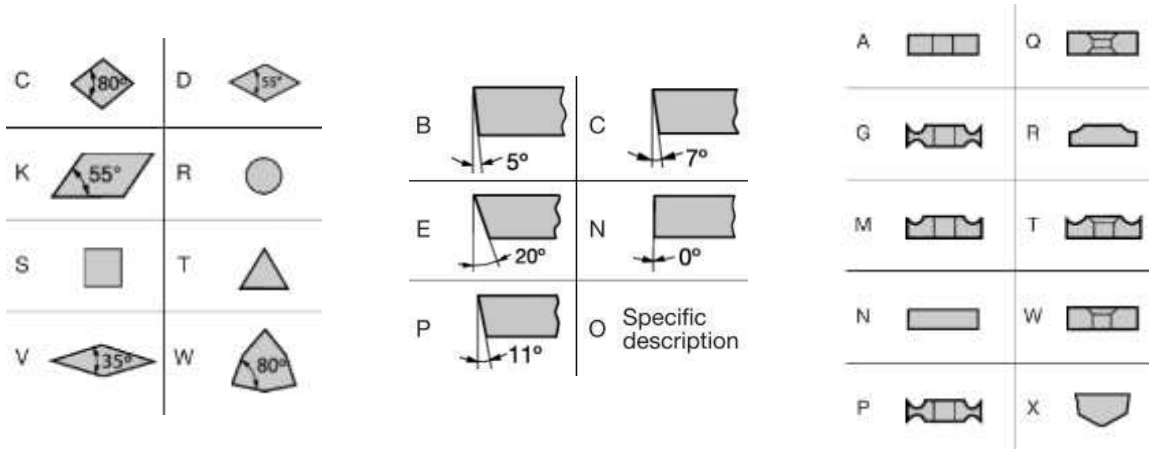

(a) First Letter (b) Second Letter (c) Fourth Letter

Figure 2.6 General Turning Insert Nomenclature [22]

The fifth number is the cutting-edge length defined by the dimension arrow of C-shape turning insert as shown in figure 2.7.

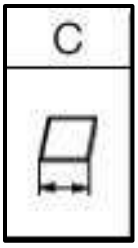

Figure 2.7 General Turning Insert Nomenclature Fifth Number [22]

The sixth number refers to the thickness of the turning insert. Table 2.1 below shows the seventh number of numeric values of the turning insert's nose radius.

Table 2.1: Corresponding nose radius with the code

Code (metric)	Radius Value
08	0.8
12	1.2

2.4.2 Cemented Carbide tools

Tool manufacturers recommend carbide, coated carbide, and coated cermet tools [21] to machine mild steels in processes ranging from roughing to finishing processes. Tools made from these materials offer good wear resistance under recommended cutting parameters. Dosbaeva et al. and manufacturer catalogues reported that the recommended cutting speed for finish cutting using carbide tools should not exceed 400m/min [14][16][21] [23]. Correa et al. reported that CVD coated carbide tools have longer tool lives than their PVD counterparts and that nose wear and chipping/fracture of the cutting edge are the typical failure modes for both coatings [24]. Khan et

al. found that although the coated carbide tool performs better than the CBN tool at lower speeds, the latter tool lasts longer when the cutting speed exceeds 175m/min for D2 tool steel [25]. This is in agreement with the manufacturer's catalogue stating that carbide tools decrease in performance as cutting speed rises.

Tungsten Carbide tools are currently used by most manufacturers with flood lubricant. [4], [26], [27]. Carbide cutting tools are widely used in the metal cutting industry to cut various hard materials such as alloy steels, die steels, high-speed steels, bearing steels, white cast iron and graphite cast iron. Sahin introduced a cutting tool coating to improve lubrication at the tool/chip and tool/workpiece interfaces, as well as reduce friction and temperatures on the cutting edge [28].

Weinert [29] reported that in dry machining of stainless steel, using carbide inserts with a Titanium Aluminum Nitride (TiAlN) coating, the higher hot hardness and strength of the tool resulted in only a small amount of flank wear and no crack formations. Higher cutting forces usually come with high temperature in the cutting zone [30].

2.4.3 CBN tools

Cubic boron nitride (CBN) and ceramic tools are widely accepted as the best replacements for costly grinding operations of hardened steels [11]. CBN tools are usually used for hard machining applications and higher cutting speeds. CBN cutting tools were found to be superior to tungsten carbide (WC) tools. Chou et al. found that there is a limited amount of research available regarding the wear of CBN tools [31]. CBN is known for its good abrasion, thermal and chemical resistance as well as the ability to maintain a sharp edge during cutting [5]. CBN has two interpenetrating face-centred cubic lattices. With one center being composed of nitride and the other of boron atoms,

this structure consists of 25% ionic bonds, making it the next hardest substance to diamond and sharing many of its properties [8]. Investigation of the CBN tool wear mechanism during the finish turning of various hardened steels revealed that an increase in the cutting speed had the most significant effect on the tool wear rate [32].

CBN tools have been commercially used since the 1970s [33]. Mustafizur et al. report that CBN is second [34] only to diamond in terms of hardness and wear durability. It also has good thermal resistance, a high thermal conductivity coefficient and high hardness at hot temperatures [35]. CBN can be used to cut certain materials seven times faster than cemented carbide at the same wear rate [34].

However, usage of coated CBN tools during HSDM presents a challenge in terms of tool life and part quality [36]. One of the possible causes for this are the coolant properties of the workpiece's ductility. During HSM, a ductile material such as low carbon steel will yield long and continuous chips [1], which generate crater wear by adhesion. From the literature, it was found that CVD Al_2O_3 and PVD TiAlN carbide inserts are the most effective tools for machining carbon steel [4]. The figure below shows the performance of each coated carbide tool on C80 and C20 steel.

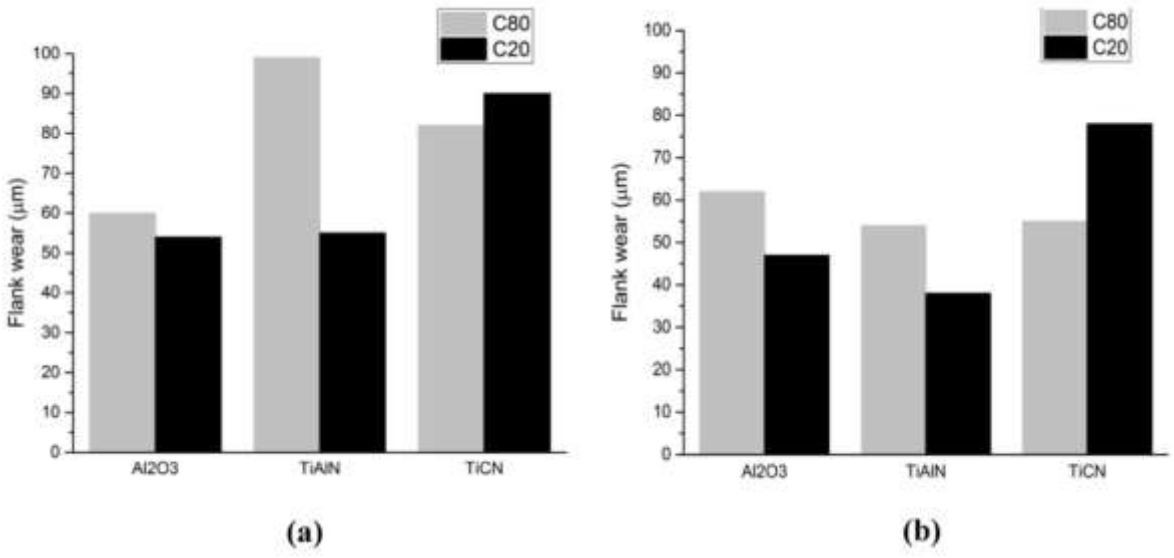

Figure 2.8 Flank wear of different coatings [4]

(a) At 600 m/min; (b) At 300m/min.

CBN is able to cut both hardened steel and hard cast iron at a high cutting speed without rapid wear [37]. Hard turning directly machines a steel part in the hardened state. This offers several benefits over grinding in some applications [19]. The cutting tool meets the following requirements: high indentation hardness, thermal conductivity, abrasive wear resistance as well as thermal, physical and chemical stability [19].

A CBN tool was selected for the HSM of low carbon steel, since it is the second hardest tool to PCD. Goindi et al. reported [6] that PCD tools are not suitable for machining ferrous based materials as the carbon atoms will rapidly diffuse into the iron chips at temperature above 700 degree Celsius, causing accelerated tool wear. CBN was also chosen for the high-speed dry machining of cast iron [6]. Since it is difficult to maintain the hardness and strength of the CBN tool at high cutting temperatures [20], coated CBN was selected for the tests whereas uncoated CBN and carbide tools were used as a reference.

A CBN insert can be very expensive and thus contributes significantly to machining costs. CBN tools have good hardness and wear durability and also feature high thermal resistance, coefficient of thermal conductivity and hot hardness [19].

CBN is formed from boron and nitrogen which form a very stable compound, BN, using the reaction shown below:

BCl3 + NH3BN + 3HCL [19]

The product formed, hexagonal boron nitride (HBN), is then transformed into CBN by the application of a high temperature and pressure. The CBN tool is made up of a collection of CBN particles which can have a range of grain sizes and are held together by a binder typically cobalt. While forming the tool solvent/catalyst can be employed, and the binder phase, degree of sintering, particle size distribution and the presence or absence of inert ceramic, metallic, or non-metallic fillers can all be adjusted to get specific properties. All CBN characteristics are affected by grain size, the percentage of CBN and its type of binder. Wyczesany et al. reported that the mechanical strength of the CBN-TiN and CBN-TiC phase, the decreasing volume of TiN and the TiC reaction to form B and N, would increase the hardness of CBN/TiN and CBN/TiC composites during post-sintering heat treatment [38]. For high CBN content tools providing higher hardness according to the literature review [39]. The hardness of the CBN materials prepared with the Al binder is predictably high due to the hard CBN phase. McKie et al. reported that the hardness decreases along with increasing CBN grain size and binder content [39]. The decrease in the CBN grain size before and after sintering is caused by crushing during mixing and the reactive sintering of the materials [39]. The figure 2.9 below shows an example of a CBN microstructure along with its grain size and binder material.

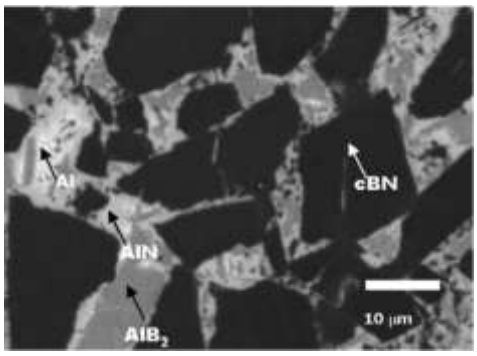

Figure 2.9 Microstructure of G20cBN25, showing the phases present [39]

According to Huang et al. [40], the figure 2.10 below shows a simple model of the abrasive-adhesive wear process with the interaction of a transferred layer. Abrasion marks are left by the CBN particles adhered to the transferred layer, which is the workpiece material. Wear mechanisms involved in CBN hard turning could be abrasion, adhesion, or diffusion, depending on mechanical and thermal loading during machining, CBN content, binder phase and chemical stability of CBN tools, and composition of the workpiece material.

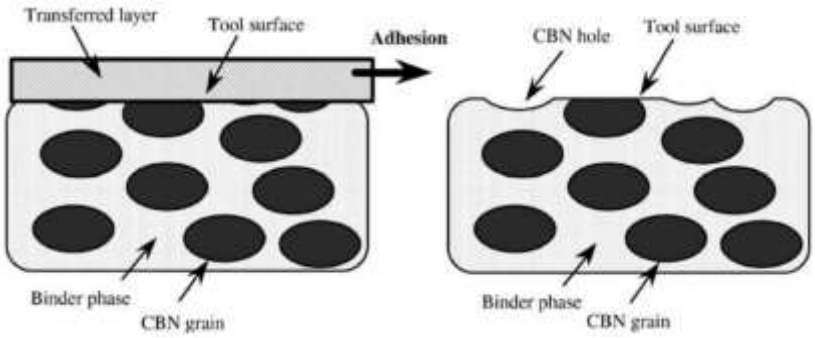

Figure 2.10 Simple mode of adhesive wear process with the interaction of a transferred layer [33]

Huang et al. reported that wear resistance increases monotonically with decreasing CBN grain size for hard turning of steel [40]. Although CBN particles and binder phases such as TiN are harder than carbides, it is still possible that the tool will encounter "soft" abrasive wear in steel machining from Sahin's report [32]. The results indicated that CBN tools with low content performed consistently better than the tools with high CBN content. The flank wear rates were related to the cutting speed, and high CBN tools exhibited faster thermal wear associated with a high cutting zone temperature [32].

Since CBN tools transfer generated heat more effectively than ceramic tools, the tool-chip interface temperature is reduced with the use of CBN tools, thus increasing the level of cutting forces. The combined capability of CBN tools to retain their hardness at high temperatures and to transfer the generated heat more effectively results in the improvement of tool life [19]. The results from Oliveira et al. show that the grades with low CBN content and the addition of a ceramic phase had a tool life three times longer than that of the grades with high CBN content [41]. Flank wear formation was mostly caused by abrasion and less by adhesion [42].

2.5 Wear, Coating, and Tribofilm

2.5.1 Tool wear criterion and mechanism

Narasimha et al. defined tool wear as the change in the shape of the tool from its original shape during cutting caused by gradual loss of tool material or deformation [43]. According to the ISO standard for a typical machining process, the failure criterion is 300-microns of flank wear for single-point turning tools [44]. Luo et al. [45] characterized flank wear as one of the most important guidelines for tool wear research. One definition of a worn-out tool is: "A tool is considered to be

worn out when the replacement cost is less than the cost for not replacing the tool" [45]. The wear mechanism can be separated into two major categories: abrasion and adhesion. Depending on the wear location and type of reaction, abrasion mostly occurs on the flank face of the cutting tool (flank wear).

The CBN wear mechanisms were assessed using the previous literature as a guide [5]. Chemical wear does not appear to be the main wear mechanism in the machining study involving uncoated CBN even when machining at lower cutting speeds. The main observed wear mechanism is soft abrasion [5].

Costes et al. report that for a 60% CBN tool with 2-µm grain size and a TiC binder machining Inconel 718, the dominant wear mechanisms during the cutting process were adhesion, diffusion and finally abrasion [46]. Luo et al. reported that during the machining AISI4340 hardened steel, the main wear mechanism of the CBN tools was abrasion with the binder material [45].

2.5.2 Coating method and its application

In machining, high temperatures are generated during cutting. The generated heat is dissipated into the chip, tool and workpiece. Over the years, coatings have been applied to the cutting tools that strive to reduce the friction between the tool-chip or tool-workpiece interfaces, thereby minimizing the temperature. It is important to understand how coatings interact with different combinations of cutting tools and work materials as well as the effect they have in the cutting region. Figure 2.11 illustrates the influence of a coating during cutting. Coatings, therefore, should be designed in such a way that they are able to withstand harsh machining conditions, provide lubricity and wear resistance and serve as a thermal barrier.

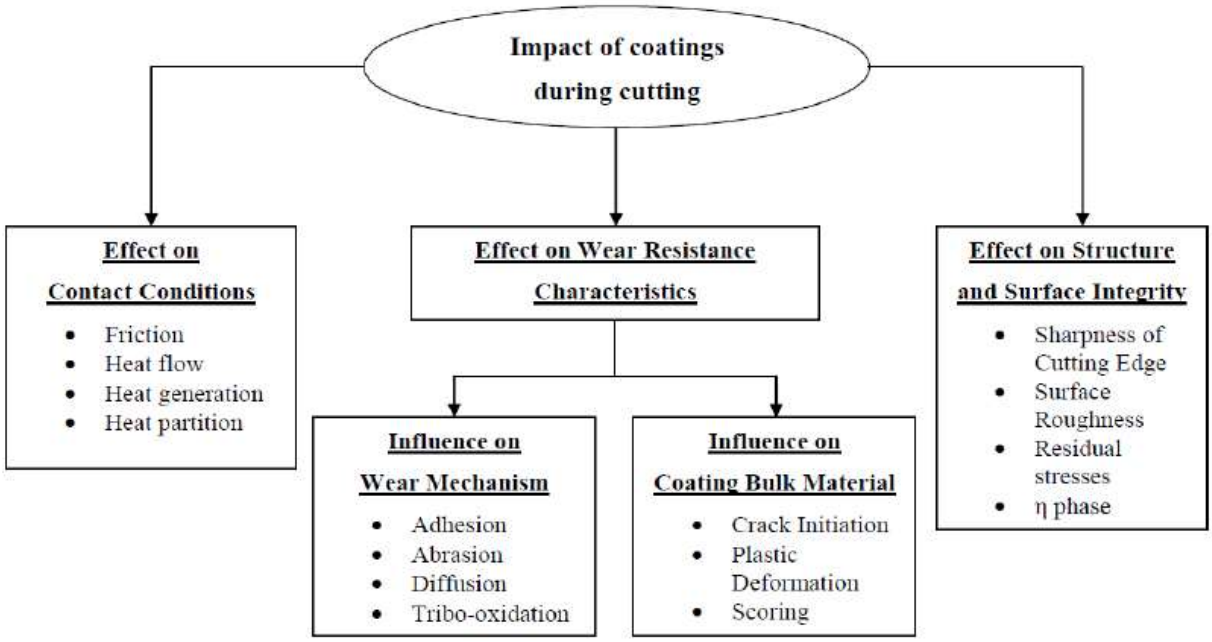

Figure 2.11 Influence of the coating during cutting [47]

Generally speaking, there are three major layers on the interface between the coating and the substrate. The first layer is the interface between the tool substrate and the coating. The chemical and physical compatibility of the coating, the thermal coefficient of expansion and the adhesion of the coating with the substrate material are of paramount importance in this layer. The second layer is the coating bulk material. The coating properties are determined by the coating composition and microstructure. The third layer is the top or outer layer of the coating. This layer determines how the coating will interact with the workpiece or the surrounding environment. Figure 2.12 shows the influences and characteristics of the coating, interface, and the substrate.

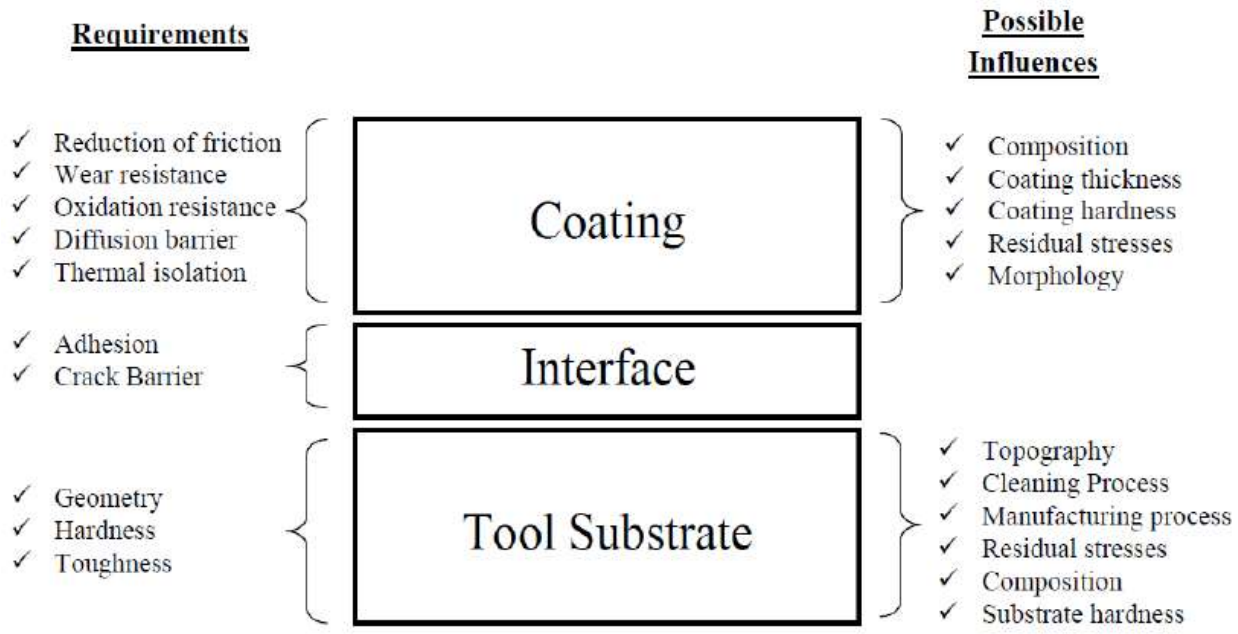

Figure 2.12 Influence and characteristics of coating, interface and the substrate of a tool [47]

Chemical vapour deposition (CVD) and physical vapour deposition (PVD) are two kinds of coating deposition techniques commonly used in industry. CVD coatings are generally thicker than PVD coatings (1-10 μm) [48] due to the different mechanism of the deposition technique. PVD is a vacuum coating process where the deposited material is evaporated from a target through arc evaporation or magnetron sputtering methods. Vaporized particles then condense to form a film on a specified substrate, such as a cutting insert. Deposition of chemical compounds is achieved by reactive gases (oxygen, nitrogen or hydrocarbons) containing desired reactants, which then react with the metal from the PVD source, or by using a similar source material [36]. To ensure uniform coating deposition, the tools constantly rotate in the coating chamber.

CVD is a heat-activated process, during which gaseous chemical compounds are introduced in the chamber where they decompose or react with appropriately heated and prepared tool substrates.

Anhydrous and anaerobic environments at sub-atmospheric pressures are often maintained inside the chamber. A uniform thick coating is formed with a refined grain structure that is dependent on the deposition temperature.

CVD coated tools are better suited for abrasive materials during the turning process, since CVD produces thick coating layers at high rates of deposition. PVD coated tools are more suitable for medium finish and finish machining processes as the cutting edge radius can be better controlled. Since PVD coatings are usually thin, it is relatively easy to control the thickness of the coating on the tool's edge. Unlike PVD coating films, CVD coatings chemically interact at high temperatures with the substrate, causing it to become more brittle. PVD coated tools tend to have a high intrinsic hardness and beneficial compressive stresses, enabling them to resist crack initiation. Furthermore, PVD coatings can also be removed from the surface of the tool, making re-sharpening them much easier, thereby reducing long term production costs [49].

Coatings can be classified into different groups. The two different types of coatings used in this thesis are shown below [49] [50] [51].

Multi-Component Coatings

These coatings can be categorized as having binary, ternary, quaternary or multiple components in their coating structure. The most successful and commonly used binary component coatings are TiC and TiN. Adding metal and/or metalloid components may improve the performance of the binary coatings. The addition of varying compositions of Al or Carbon Nitrides creates ternary coatings. Improvements of ternary coatings are dependent on the working conditions. No quaternary and above coatings were used in this research.

Multiple-Layer Coatings

These coatings are deposited on top of each other with different functional layers positioned in between. The goal is to incorporate multiple properties and characteristics in the assembled coatings. The outer layers of the multi-layer coatings typically provide friction and wear resistance, while the inner layers enhance adhesion resistance, arrest cracking, even out stress, support load and stop diffusion. A well-known multi-layer coating for carbides is TiC-Al_2O_3-TiN. The TiC layer has a similar thermal coefficient to cemented carbides, thereby increasing the adhesion of the coating to the substrate. The low thermal conductivity of the Al_2O_3 layer protects the substrate from heat during cutting while the outer TiN layer provides enhanced wear resistance over the base tool material.

Fox-Rabinovich and Kovalev reported that a single chamfered cutting edge is optimal for tool wear reduction, since it is reinforced without significantly affecting mechanical and thermal loads. The main wear mechanism observed at all micro geometries was attrition [52]. A study of wear mechanisms and tool performances of TiAlN PVD coated inserts during the machining of AISI4140 steel at high speeds under both dry and wet machining found that dry cutting performed better than wet cutting at speeds of around 200-400m/min [32].

2.5.3 Tribological behaviour

Tribofilms are thin films that form on the interface or worn surface during friction. They are dynamic structures that have a different chemical composition as well as tribological and structural characteristics from the underlying bulk material [51] [53]. They have been shown to have a significant influence on the frictional characteristics and wear performance of tools.

Three main mechanisms responsible for tribofilm formation are suggested to be:

(1) mechanical grain refinement arising from severe plastic deformation, (2) thermally-induced phase transformation due to high cutting temperature, (3) surface reaction with the environment. Tribofilms provide a thermal barrier (protection) and lubricating functions [54]. Tribofilms can affect tool tribological performance, corrosion resistance and fatigue life [19]. Aizawa et al. reported that TiCN material can form a tribo-layer or protective layer such as TiO, TiN, and TiC which can decrease the friction coefficient at the machine surface. SiO and MnO are also present on the cutting tools tested in this study [55].

The application of coatings has been shown to improve the tribological properties of tools during metal cutting in the following ways:

1. Improved wear resistance upon increasing cutting speed.

2. Reduced friction can assist in cutting-zone temperature control, which may even lead to the elimination of cutting fluid.

3. Reduced the tendency of sticking and material adhesion to the machined surface, such as BUE formation [48]. The increase of tool life alongside the cutting speed in CBN could be due to the formation of a protective layer on the chip-tool interface [45].

2.6 Summary

The literature review recommends the use of carbide tools for low carbon steel machining due to its good performance at lower cutting speed (120-440 m/min). CBN tools are usually used for hardened steel (hardness greater than 45 HRC) machining [11]. Dry machining has been successfully implemented only for a few workpiece materials and machining operations such as

dry milling and dry turning of cast iron and some titanium alloys. HSM of low carbon steel could potentially deliver a more productive and sustainable manufacturing process. To implement HSDM using CBN on LCS, factors such as cutting speed, feed, DOC, cutting force, cutting zone temperature, tribo-film formation, BUE formation, surface finish and tool life needed to be studied. HSDM for low-carbon steel using CBN tools was a gap in the literature for current machining practice that this research addressed.

3 Methodology and Experimental Outline

3.1 Workpiece

AISI 1018 used in this study is a type of plain carbon steel with trace amounts of other elements. AISI 1018 is malleable and easy to machine. The chemical composition of low carbon steel and the mechanical properties of AISI 1018 steel are given in Table 3.1.

Table 3.1: Chemical composition and mechanical properties of AISI 1018 steel [56]

Chemical composition (%)					
C	*Fe*	*Mn*	*P*	*S*	
0.14-0.20	98.81-99.26	0.60-0.90	Max 0.040	Max 0.050	
Mechanical properties					
Yield Strength	*Tensile Strength*	*Elongation at Break*	*Modulus of Elasticity*	*Shear Modulus*	*Hardness Vickers*
370 MPa	440 MPa	15%	205 GPa	80 GPa	131 HV

The microstructure of AISI 1018 performed by etching the sample with 5% nital etchant is shown in figure 3.1, it can be compared to figure 2.2 low carbon steel. Low carbon steel contains mostly ferrite (65%) and pearlite (35%). Ferrite is a soft structure and pearlite is a very fine lamellar mixture of ferrite and cementite. This property is what makes AISI 1018 easy to machine, as well as prone to BUE formation.

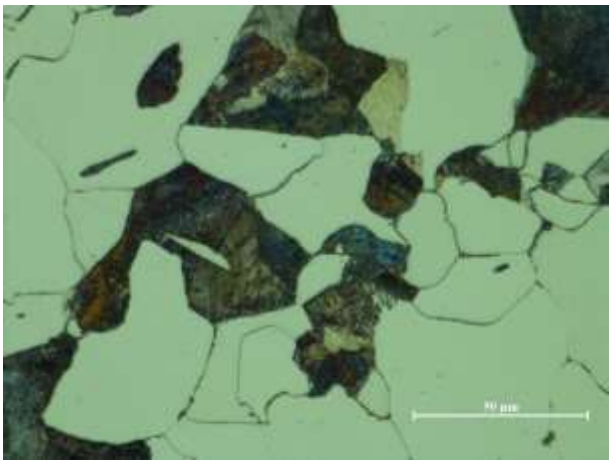

Figure 3.1 Microstructure of AISI 1018 steel at 50x, 5% Nital Etch

3.2 Tool Selection

All the tools selected for this comprehensive study are commercially available coated and uncoated tools from Kennametal, Sumitomo, Tungaloy, and Nikko. Post-treatment and coating development could be included in future studies.

According to the ISO standard mentioned in 2.4.1, the selection of CBN cutting tools [CBM(G)A120408] is: Rhombic type insert 80 degree (C), relief angle of 0 degree (N), Tolerance class of (M) or (G), with cylindrical hole without chip breaker (A), 12.7mm inscribed circle size (12), thickness of 4.76mm (04); corner radius of 0.8mm (08).

The table 3.2 below shows the tools used in the study. B0 was the benchmark tool coated carbide. U_i represents the uncoated tools, and the coated CBN tools were labelled as C_i., where the subscript "*i*" represents a similar tool substrate (binder material, grain size, percentage of CBN content). The coated carbide tool is used in the benchmark study.

Table 3.2: Selected Cutting tools

Label	Tool Grade	ISO Standard	Description	Binder Material	CBN Content (Carbide)	Hardness (HV)	Grain Size (µm)	Coating
B0	KC 730	CNMG 120408	General-purpose machining of steel, notch, BUE resistance, run at the higher speed [57].	N/A	Carbide	N/A	N/A	Al2O3-TiN
U1	KB 1340	CNMA 120408	Solid CBN insert having multiple cutting edge [58].	N/A	High	N/A	10	-
C1	KBK 35	CNMA 120408	Coated CBN insert having multiple cutting edges.	N/A	High	N/A	10	Al2O3-TiN
U2	BN 350	CNMA 120408	Highest fracture resistance and toughest CBN. heavy interrupted cutting conditions.	TiN	60-65	33-35GPa (3365-3569)	1	-
C2	BNC 300	CNGA 120408	The tough grade for heavy interrupted cutting applications.	TiN	60-65	33-35GPa (3365-3569)	1	TiAlN based coating
U3	BN 1000	CNMA 120408	Best wear resistance grade, high-speed continuous cutting	TiCN	40-45	27-31GPa (2753-3161)	1	-
C3	BNC 2010	CNGA 120408	Finishing with good surface roughness and dimensional accuracy [16].	TiCN	50-55	30-32GPa (3059-3263)	2	TiCN multi-layered coated tool
U4	NBL 350U	CNGA 120412	Uncoated insert for interrupted cutting condition	TiN	75	3200	1-2	-
C4	NBL 350C	CNGA 120412	Coated insert for interrupted cutting condition [23].	TiN	75	3200	1-2	AlTiN
U5	BN 2000	CNGA 120408	General-purpose grade for hardened steel that provides a high fracture and wears resistance. [16]	TiN	50-55	31-34GPa (3161-3467)	2	-

The coated carbide tool is the benchmark tool used to machine low carbon steel at a recommended cutting speed of 200m/min. Out of the selected testing inserts, B0 is the only tool with an embedded

chip breaker and a positive cutting angle. The chip breaker is used to break the continuous chip formed when machining mild steel.

Figure 3.2 Coated Carbide insert preview Cutting edge of B0

All coated and uncoated CBN tools (U1 to U5 and C1 to C4) were selected to have a similar geometry. Since chip breakers and positive cutting angle features are hard to find in commercially available CBN tools, CNMG120408 was used. The corresponding geometry representation information can be found in the literature review section.

The image below shows four unused coated CBN tips with their corresponding grade. The C1 coated tool is a solid CBN tool, whereas C2, C3, C4 are CBN tips embedded within a carbide tool body.

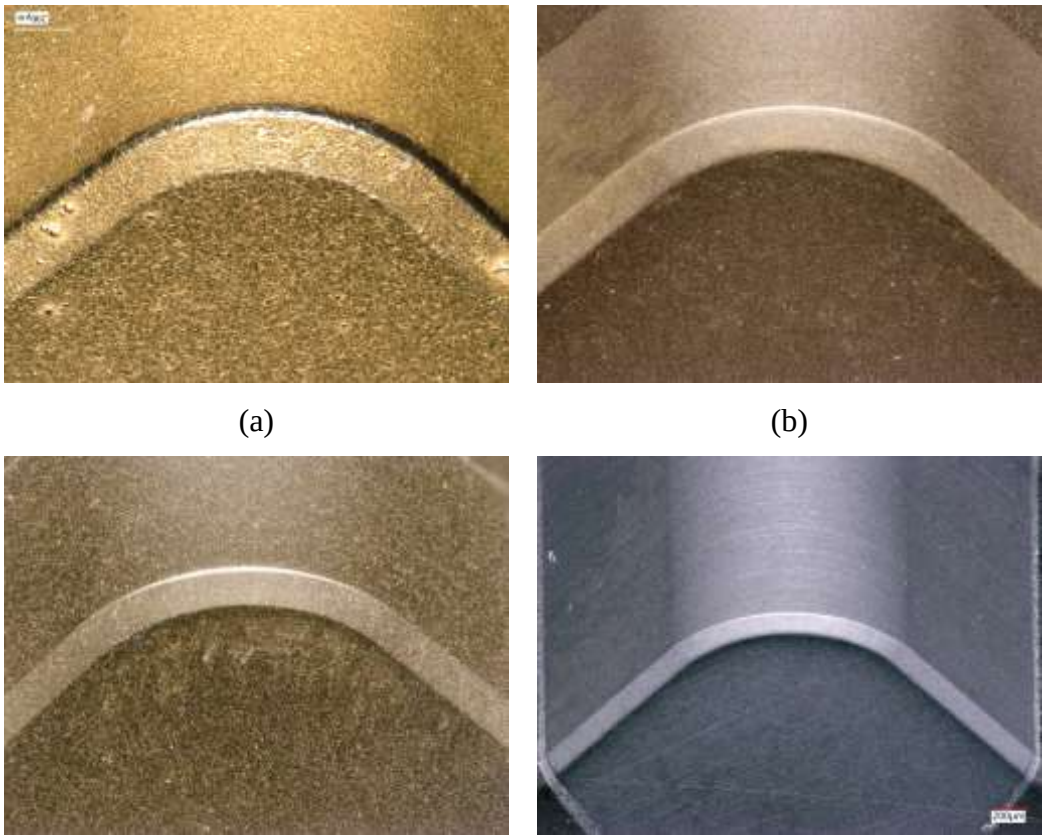

(a) (b)

(c) (d)

Figure 3.3 Coated CBN inserts preview from Microscope: Cutting edge of (a) C1, (b) C2, (c) C3, (d) C4

Figure 3.4 below shows the uncoated CBN tools selected from various manufacturers, along with the grade, and properties as indicated. The substrate composition and coating material composition vary with grade number. Only one uncoated CBN U1 is a CBN tool, all other are CBN tips embedded with a carbide body.

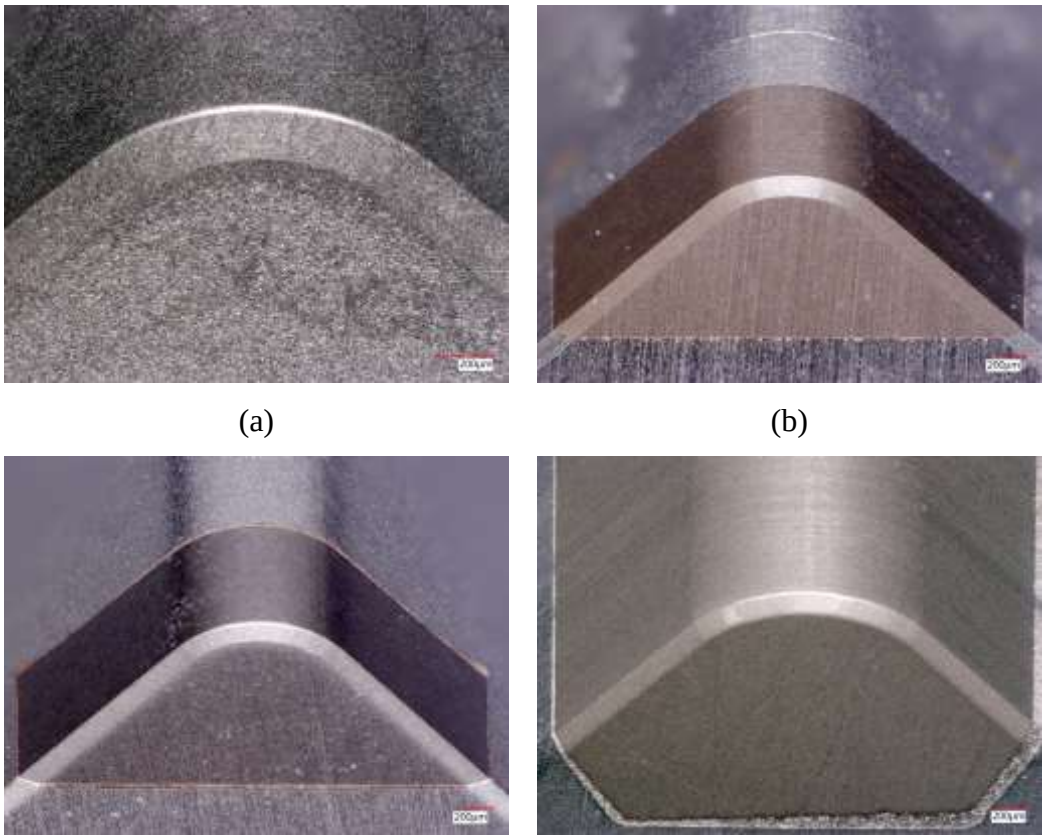

(a) (b)

(c) (d)

Figure 3.4 Uncoated CBN inserts microscope preview from: Cutting edge of (a) U1, (b) U2, (c) U3, (d) U4

The image above depicts the tool conditions before experimenting. The insert is first surveyed by the Keyence microscope, and then a cutting-edge measurement is performed with a different orientation to observe the wear progression.

3.3 Machining Setup

The experiment was conducted using a Boehringer CNC lathe machine (VDF 180), with maximum spindle speed of 4200RPM. The tool holder was DCLNE 16 4D from Kennametal. After each

machining test pass, the wear was measured using a Keyence optical microscope. The length of each pass depended on the tool life of each specific test, varying from 10 meters to 1000 meters per pass. The experimental set-up is shown in Figure 3.5 below.

Figure 3.5 Machining set up in Boehringer three-jaw clamps, cylinder shape of AISI 1018, Coated carbide insert B0

3.4 Experimental Methodology

Step 1: **Tool Edge geometry measurement:** Cutting edge geometry was validated using the Alicona infinite Focus system (white light interferometer microscope) prior to the machining process as shown below in Figure 3.6.

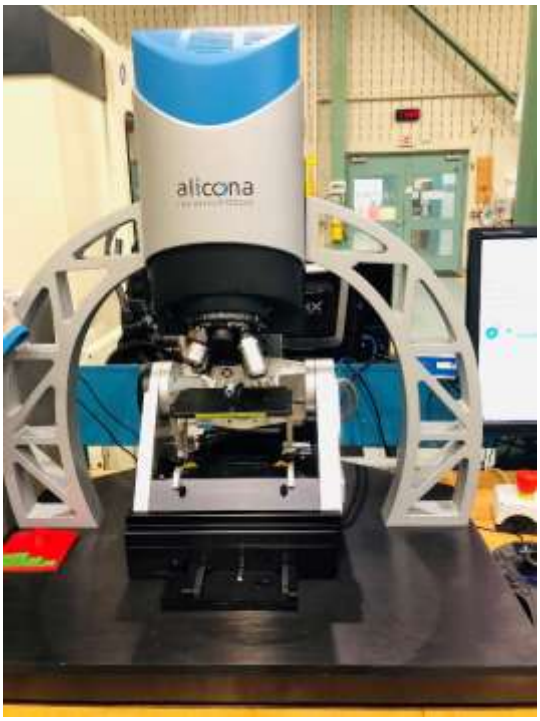

Figure 3.6 Alicona INFINITEFOCUS light interference microscope

Step 2: **Hardness and Residual stress measurement**

The hardness of the CBN insert was measured using an indentation test performed using a CLEMEX CMT.HD microhardness tester as shown in figure 3.7. A Vickers indenter was used to measure the HV value. A further value of HRC was derived from the HV value given by the device.

Figure 3.7 CLEMEX intelligent – CMT High Definition microhardness tester

Step 3: **Tool Wear Analysis----Flank wear measurement using Keyence microscope**

The cutting tool was examined using a Scanning Electron Microscope (JOEL 6610LV) to investigate the cutting-edge wear mechanisms and using a Keyence digital optical microscope (VHX 5000) to study the wear mechanisms on the flank faces of the cutting tools. The surface speeds were 500 m/min and 1000 m/min, feed rate was 0.15 mm/rev and the depth of cut was 0.3 mm.

Wear measurement after each pass

Wear analysis was performed using the Keyence microscope after each pass of the machining process. At the end of the tool life, the final tool life was recorded as the length of cut. Multiple wear types were observed on the tool during machining, especially flank and crater wear.

Workpiece properties, coating composition, and machining parameters were considered as variables which may affect the tool life.

Step 4: **Machined Workpiece Analysis----Surface roughness of the machined surface:**

The surface roughness of the machined workpiece was measured and calculated using a hand-held roughness tester shown in figure 3.8. A measurement was taken once the device was stabilized. Ra and Rz were extracted from each analysis.

Figure 3.8 Mitutoyo SJ-201 handheld surface roughness tester, Boehringer lathe, cylinder shape of AISI 1018

Step 5: **Coating characterization**

All the coated tools were inspected and characterized after the machining process. The fracture cross-section was observed using a white light-interferometer microscope as shown previously in figure 3.6. The machined inserts from Step 4 at the end of the tool life were observed using a

scanning electron microscope (SEM). The purpose of this step was to verify the material specifications given in the manufacturer catalogue and to assess the coating performance.

Step 6: **Sampling, Polishing using Abrasive saw and Polisher**

The workpiece material sample was extracted using an AbrasiMatic 300 abrasive cutter shown in figure 3.9. The sample obtained was then placed into the mounting equipment.

Figure 3.9 AbrasiMatic 300 Abrasive cutter

The hot mount equipment, as shown in Figure 3.10 below, was used to position the sample in preparation for the polishing process. Black phenolic thermosetting powder was used to hold the sample (workpiece material and cutting inserts) during the polishing process.

Figure 3.10 Struers CitoPress-20 and MetLab METPRESS 2A Hot Mount machine with Black Phenolic Thermosetting powder

The mounted samples were placed within the auto polisher shown in figure 3.11 under the following specifications (CBN Polishing process: SiC-Paper#220 for 1:30 min; SiC-Paper#500 for 1:30min; Plan DP-A 15 µm for 5:00min; Plan DP-A 9 µm for 5:min; Dur DP-A 3 µm for 4:00 min; Chem 0.05 µm with OP-S for 2:00 min)

Figure 3.11 Struers Tegramin-25 Auto polisher

Step 7: **Grain size, Binder material, Percentage CBN obtained by SEM**

A Nikon DS-F12 Microscope shown in figure 3.12 was used to measure the microscopic structure of the workpiece material following the etching process. A JEOL6610LV SEM instrument in figure 3.13 was used to perform SEM and EDS imagery. The range of magnification was between 500x-4000x depending on the purpose of the image. XRD equipment was used to analyze the elemental phases found in EDS.

Figure 3.12 Nikon DS-F12 Microscope

Figure 3.13 JEOL JSM-6610LV SEM device

Step 8: **Data analysis Image J, FEA and wear curve forming**

Image J data analysis software was used to analyze the SEM and EDS images. Multiple measurements were made to obtain the average grain size of each cutting tool.

FEA simulation was performed using AdvantEdge software. The simulated force was compared with the force measured by the dynamometer to obtain an estimate of the cutting zone temperature where the agreement of force between the model and the experiment were used to build confidence in the temperature estimate.

Step 9: **Repetition of Step 1 to Step 7 for each designed experiment.**

3.5 Experimental Design

To understand how CBN tools interact with the workpiece material, the following preliminary test was carried out (Table 3.1). Coated CBN tools were compared with coated Carbide Tools at cutting speeds as outlined in Table 3.3. The recommended cutting speed from the literature is 150m/min – 300m/min DOC 0.3 and Feed 0.15 mm/rev for carbide tools during the finish turning process [14][15][16]. The high-speed region of low carbon steel varies from 400 m/min to 1400 m/min. The following high-speed cutting condition was selected for machining low carbon steel with CBN tools. A fixed feed rate, and depth of cut (DOC) and surface speed was used throughout this study.

The performance of coated carbide, uncoated and coated CBN tools during the machining of low carbon AISI 1018 steel is compared in table 3.3 at cutting speeds of 500m/min and 1000m/min.

Table 3.3 Cutting condition and parameters for each tool.

Surface speed	Feed	DOC	B0	U0	C1
500 m/min	0.15 mm/rev	0.3 mm	Dry/Wet	Dry	Dry/Wet
1000 m/min			N/A	Dry	Dry/Wet

The cutting conditions and parameters from table 3.4 were found using the results from performing the testing outlined in table 3.3 to compare the benchmark tools (Coated Carbide) with a selected

coated CBN tool using the same coating and cutting speed (500m/min), but under different cooling conditions. The test results included different cutting conditions (dry and wet) under the same cutting parameters. This experiment revealed whether the coated CBN could outperform the benchmark cutting insert in terms of the tool life and surface integrity.

Table 3.4 Cutting condition and parameters of the Uncoated CBN tool.

Substrate material	B0	B0	C1	C1
Cutting condition	Dry	Wet	Dry	Wet

Table 3.5 below shows the conditions and cutting parameters of the cutting speed test, using the same U1 uncoated CBN tool. The effect of cutting speed on the tool wear can be observed at different cutting speeds. The primary wear interaction between the uncoated CBN and the workpiece material is reviewed.

Table 3.5 Cutting speed used on U1 with Feed 0.15mm/rev and DOC of 0.3mm.

Surface speed (m/min)	400	500	600	700	800	1200

Table 3.7 is a focused study (Study A) of different uncoated CBN tools, in which the properties vary due to the differences in binder material, grain size and percentage of CBN content. The study

reveals the effect of uncoated CBN properties on tool life and part quality. A suitable cutting speed of 500m/min was selected based on the previous test. All of the following tests were conducted under the same cutting conditions shown in table 3.6.

Table 3.6 Cutting conditions

Surface speed (m/min)	**Depth of cut (mm)**	**Feed rate (mm/rev)**	**Coolant state**
500	0.3	0.15	Dry

The binder material is given in Table 4.2 for the selected tools and coating information is provided in table 3.2.

Table 3.7 Cutting tool used in Study A (Uncoated CBN tools) with a 500m/min surface speed, Feed rate of 0.15mm/rev and 0.3mm DOC.

Tools	U1	U2	U3	U4	U5
Substrate Material	Al	TiN	TiCN	TiN	TiN
Grain Size	10	1	1	1	2

Table 3.8 is a focused study (Study B) of different coated CBN tools. The substrate of the selected sample is expected to be similar to that of the corresponding uncoated CBN tools in Study A. The goal of this experiment was to validate the test result from Study A and to verify the effect of the coating material on the tool life.

Table 3.8 Cutting condition and parameters of Study B (Coated CBN tools).

Tools	C1	C2	C3	C4
Coating Material	Al2O3	TiAlN	TiCN	AlTiN
Grain Size (μm)	10	1	2	1
Coating Thickness (μm)	15.1 ± 5.5	3.7 ± 1.3	3.4 ± 0.4	5.8 ± 1.6

At the end of this study, a coating will be selected from the Study B to be deposited on the best-performing substrate select from the Study A.

4 Tool Characterisation

4.1 Geometry

According to Table 4.1 which shows the measured edge geometry of CBN tools, U2 and C2 have the smallest mean edge radius of 7.1µm and 15. 1µm, respectively. The CVD coated C1 and its uncoated pair U1 have larger respective mean edge radius of 55.3 and 36.3µm, with a negative bevel angle of 20 degrees. All other inserts have a similar mean edge radius of around 15 µm and negative bevel angle of around 25 degrees.

Table 4.1 Cutting tool geometries and properties table

Tool	Geometry		
	Cutting edge radius	Negative bevel angle	T-land length
	r (µm)	Yb (degree)	By (µm)
B0	46.39	N/A	N/A
U0	N/A	N/A	N/A
U1	26.3	20.2	214.7
C1	55.3	19.7	237.5
U2	7.2	25.2	150.1
C2	15.1	25.2	161.1
U3	14.5	25.3	140.7
C3	16.4	25.1	138.1
U4	15.1	35.3	156.0
C4	12.9	35.1	138
U5	10.5	26.0	150.0

The edge geometry of all inserts was measured with an Alicona white light interference microscope. The measured values of all parameters for the form factor method are reported in the above list. A FEM simulation of cutting forces and temperatures was performed for the uncoated CBN tool.

4.2 Grain Size and Binder Material Analysis

Figure 4.1 below shows all SEM images used for grain size analysis of the selected tools. The images show the SEM BES analysis of all the coated and uncoated CBN tools after polishing. The grain size of each selected insert was verified with Image J software by taking the average measurement of 20 random grains from each image. The results are shown in Table 4.1.

The dark area represents the CBN grains and the bright area is the corresponding binder material of each tool. The results show that the catalogue data agrees with the measurement.

The results shown for all the measurement are presented below in Table 4.1. Each pair of CBN tools have a similar grain size.

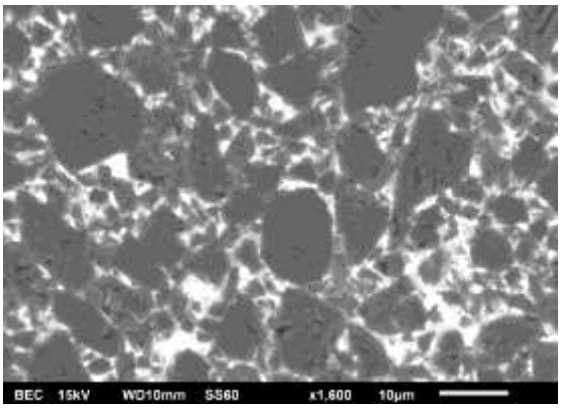
BEC 15kV WD10mm SS60 x1,600 10μm

(a)

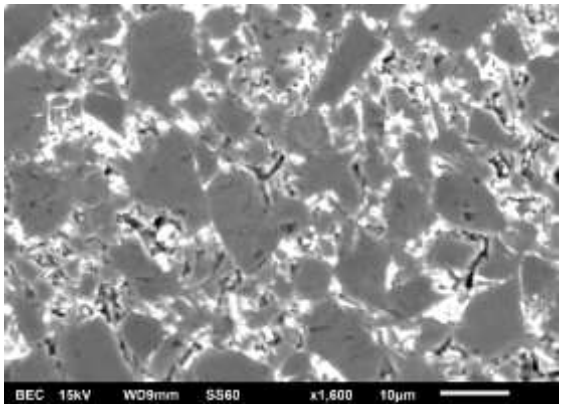
BEC 15kV WD9mm SS60 x1,600 10μm

(b)

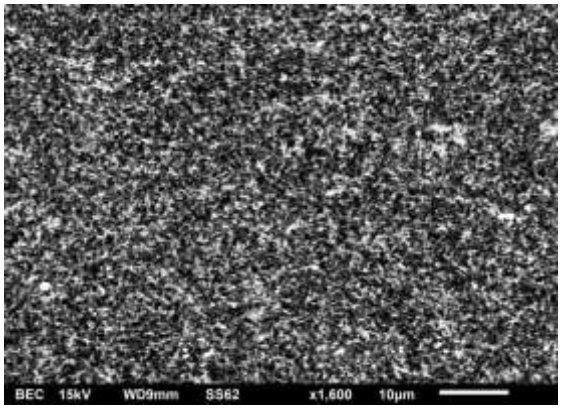
BEC 15kV WD9mm SS62 x1,600 10μm

(c)

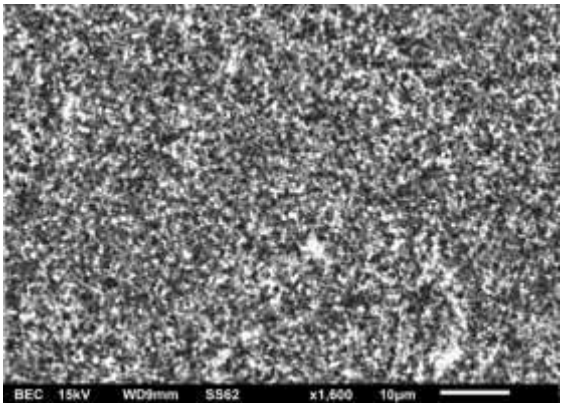
BEC 15kV WD9mm SS62 x1,600 10μm

(d)

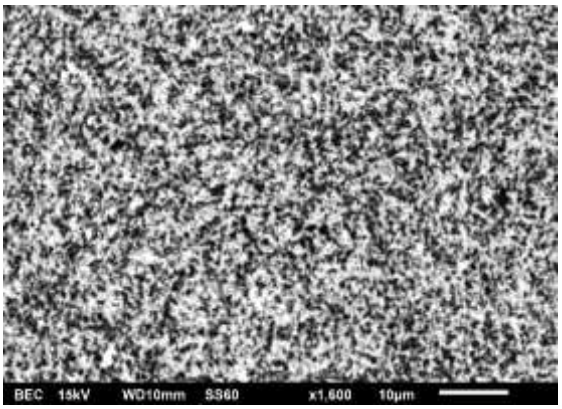
BEC 15kV WD10mm SS60 x1,600 10μm

(e)

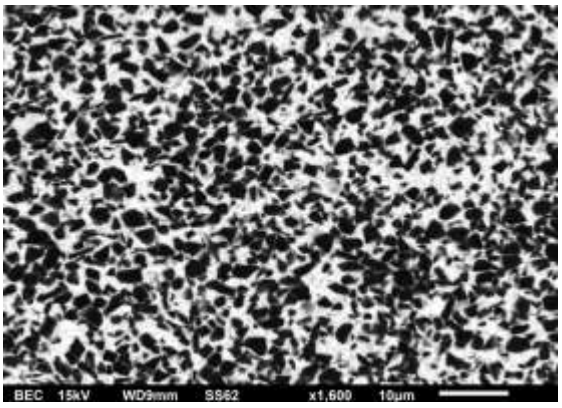
BEC 15kV WD9mm SS62 x1,600 10μm

(f)

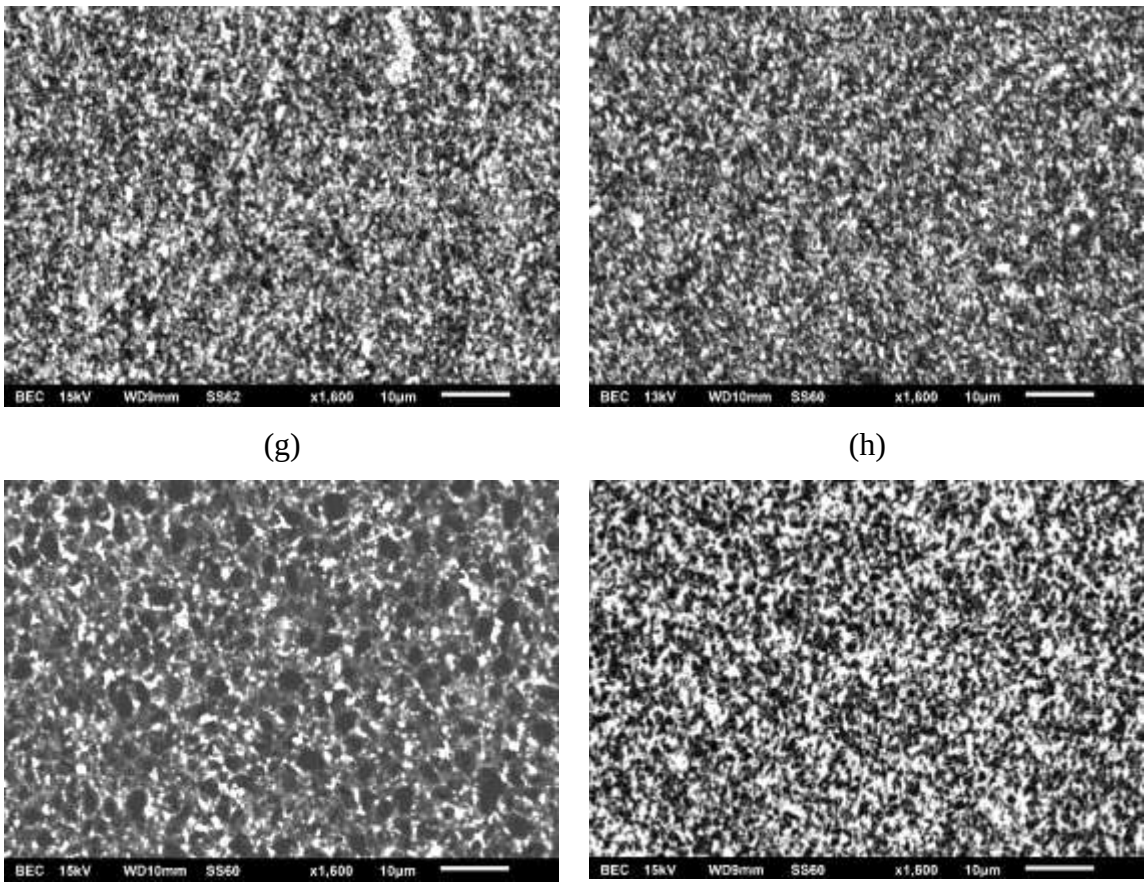

Figure 4.1 (a) U1, (b) C1, (c) U2, (d) C2, (e) U3, (f) C3, (g) U4, (h) C4, (i) U0, (j) U5 cross section at 1600x

Based on EDS data in Table 4.2 below and literature review, the binder material in U1 and C1 is Al-B or Al-N. AlB/AlN are suitable binder materials for tools with high CBN content (>90%). The hardness of the CBN tool with Al-based binder should depend on the CBN phase. The grain size was 10-microns.

EDS analysis showed the composition of binder material in U2 and C2. From the catalogue, the binder material was TiN of grain size 1 µm and the C2 coating material was TiAlN. EDS also showed that U1 and C1 contained less BN. The binder material is TiN according to the catalogue and XRD validation.

The binder material of U3 and C3 given in the tool catalogue was TiCN. The EDS result showed an excess of Ti and C in the binder material. The grain size of U3 was 1-µm, C3 2-µm. The coating material of C3 was TiCN + TiN.

Table 4.2: Grain size, hardness and SEM data and EDS analysis of binder material composition

Tool	Substrate Element EDS Analysis (%Weight)								Grain (µm)	Hardness (HV)
	B	N	Al	O	Ti	C	W	Co		
B0	-	-	-	1.1	-	8.2	86.4	4.0	2.05±0.65	1921±20
U0	43.1	41.3	1.7	2.5	-	-	4.3	6.8	2.79±0.72	4106±147
U1	50.6	41.6	7	-	-	-	-	-	9.43±3.10	5103±241
C1	48.8	44	7.2	-	-	-	-	-	8.75±2.85	5087±336
U2	37.2	32	7.1	4.7	17.9	-	1	-	0.76±0.16	4009±134
C2	35.1	31.8	7	5.4	17.6	-	2.4	0.5	0.81±0.24	4078±126
U3	25.3	21.8	5.1	4.4	33.5	8.7	0.9	-	0.82±0.27	4560±156
C3	32.1	27.9	3.4	3.5	24.9	6.1	1.6	0.5	1.64±0.88	4800±338
U4	31.8	31.2	5.0	5.2	25.8	-	0.7	-	0.89±0.35	4476±278
C4	27.6	28.2	4.5	4.8	33.6	-	0.8	-	0.84±0.28	3982±67
U5	27.9	28.9	4.2	4.2	31.2	2.8	0.6	-	1.46±0.35	4640±277

From the table 4.2 and the table 4.3 below, which shows the binder phase analysis using XRD technique, the binder material compositions were validated and given in the last column in table 4.3. Notice the binder phases were given from the tool manufacturer. After the sintering process, the binder phases will shift depending on the different process and the starting phases. Wyczesany et al. reported that binder phase can form TiO, TiC and TiN when reacting with B and N during post-sintering heat treatment [38]. From the literature Al added to the CBN tool making process

can also form AlN phase in the binder. The binder phases are major depending on the phase and percentage contain in the EDS analysis.

Table 4.3: Phases analysis using XRD for substrate material composition.

Tool	Substrate Phase XRD Analysis							Binder Phase
	WC	**BN**	**Ti (O, C, B)**	**Ti (B) N**	**Ti (C, N)**	**Al (N, O)**	**Co**	
B0	WC	-	-	-	-	-	Co	Co
U0	WC	B1.1N 0.9	-	-	-	AlN	Co	W, Co
U1	-	B1.1N 0.9	-	-	-	AlN	-	Al
C1	-	B1.1N 0.9	-	-	-	AlN	-	Al
U2	-	BN	TiO	Ti0.86B0.37 N0.73	-	Al2O3/Al2	-	TiN
C2	-	BN	-	Ti0.86B0.37 N0.73	TiC0.4N0.6/ TiC0.14N0.37	Al2O3	-	TiN
U3	-	BN	TiC/TiB	-	TiCN	Al2O3	-	TiCN
C3	-	BN	TiO(ii)	TiN0.58	Ti (C0.25N0.75)	Al2O3	-	TiCN
U4	-	BN	TiB2	Ti0.86B0.37 N0.73	-	Al2O3	-	TiN
C4	-	BN	TiB2	Ti0.86B0.37 N0.73	-	Al2O3	-	TiN
U5	-	BN	TiO(ii)	-	TiCN/TiC0.06N 0.94	Al2O3	-	TiN

It can be seen and validated that Aluminum is added to CBN sintering process for all coated and uncoated CBN tools. Binder materials formed different phases due to the temperature and sintering process differences, which will affect the tool performance.

4.3 Summary of Tool characterization results

The selection of the CBN tools was based on their grain sizes and binder material composition. Each pair of tools has the same substrate properties, with one being coated and the other uncoated. The final selection of CBN tools is shown below in Table 4.6 with other characteristics such as hardness and geometry analyzed by the available equipment.

It can be seen in Table 4.2 that U3 has the highest HV hardness value out of the six selected CBN tools. Each pair of CBN tools have a similar hardness range, binder material, grain size and design. The experiment below will define the effect of each property during the machining of the workpiece material.

5 Results and Discussion

This chapter presents a summary of this comprehensive study from various aspects. It refers to the experimental methodology, experiment design, and the machine set-up from Chapter 3 and 4. The experimental results are shown below in the benchmark study, study A (Uncoated CBN tools) and study B (Coated CBN tools), followed by discussion and analysis of each result.

5.1 Benchmark study

5.1.1 Coated carbide vs Coated CBN

The benchmark tool is compared with the target tool (composed of coated tungsten carbide and coated CBN, respectively) in terms of tool life under different cutting conditions.

The tool life failure criterion is flank wear reaching 300-µm wear for the selected coated carbide B0, coated CBN C1 and uncoated CBN U0 under various cutting conditions (500m/min and 1000m/min cutting speed; dry cutting condition and wet cutting condition).

The results in Table 5.1 show that the tool life of the coated CBN C1 is comparable to B0 at 500m/min. In the B0 tool, tool life is improved with coolant use. However, the tool life of C1 is better under dry conditions. This may be due to the thermal shock caused by the coolant at the tool-workpiece interface. The CBN tool is thus expected to have greater cutting force. According to the design of C1 has no chip breaker, and B0 has a embedded chip breaker with the same rake angle of 5 degrees.

Table 5.1 First test of cutting tool parameters and corresponding tool life in meters.

Cutting condition	**Tool life (meters)**	
	B0	**C1**
500 m/min, Dry	9335	12284
500 m/min, Wet	10188	11848

Figure 5.1 shows the C1 wear curve and performance of the B0 tool at 500m/min under dry and wet cutting conditions. Figure 5.1 indicates that the tool life is improved by 16.3% (wet-wet condition) and 31.6% (dry-dry condition) when using C1 rather than B0 inserts. The coated CBN tool outperformed the coated carbide tools in terms of both tool life and surface integrity of the machined parts (Ra 1.6 and below for coated CBN, Ra 1.6 and above for coated Carbide). This result also reveals that dry cutting is applicable for machining AISI 1018 low carbon steel using a coated CBN tool, since the tool life performance of dry cutting with the C1 tool is 20.6% better than that of B0 in wet condition.

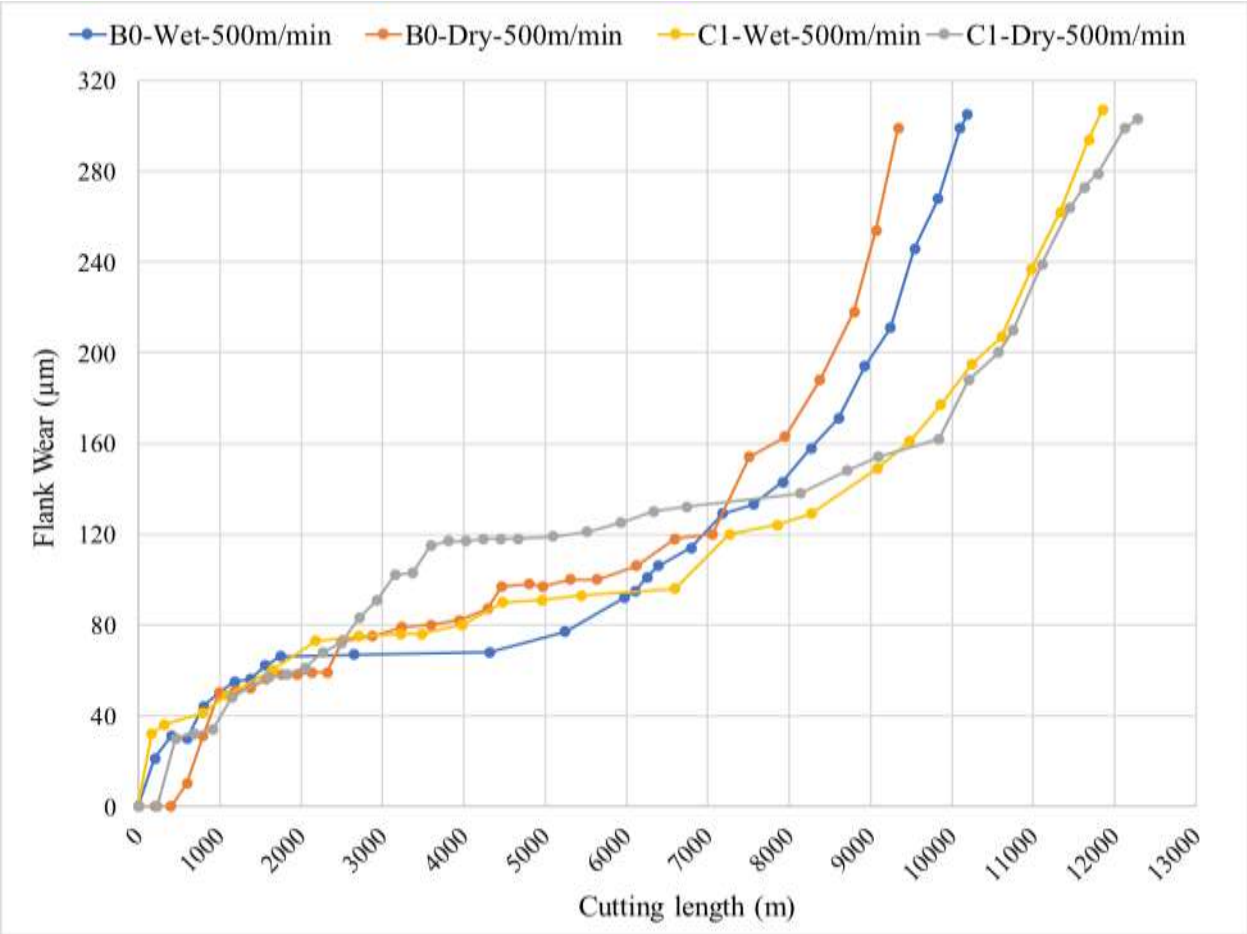

Figure 5.1 B0 and C1, Wear vs. Cutting length Comparison of Coated Carbide and CBN tool life at 500 m/min

Figure 5.2 below shows the final flank wear of 303 µm that appears after 9335 meters of cutting without coolant using a coated carbide B0 tool. BUE could be observed and tool wear is more localized under the dry condition. A final flank wear of 305 µm appears after 10187 meters of cutting with coolant using B0 (b). The tool life is longer, and wear is less localized. Less adhesion occurs during the final stage of the machine test.

It was observed that in B0, use of coolant prolongs tool life by reducing thermal localization and BUE.

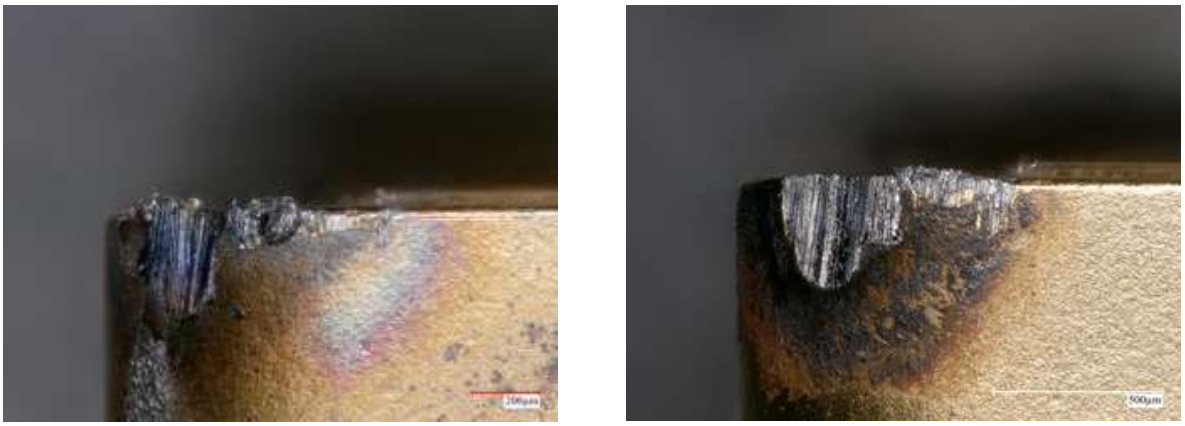

(a) (b)

Figure 5.2 PVD coated Carbide after (a)9335m of dry machining, (b) 10187m of wet machining

Under the wet cutting condition, the tool life is 9% better in the coated carbide insert than under the dry cutting condition, which falls within the margin of error and does not show major improvement. Built-up-edge formation occurred during the experiment. A study by Goindi and Sarkar reports that in dry cutting, low carbon ferrous alloys tend to feature BUE [6]. Figure 5.2 shows that at the end of the experiment, wear is more localized under dry cutting due to high cutting zone temperature. The wear mechanisms were mainly abrasion and adhesion under the wet condition.

The SEM (Figure 5.3(a)) and EDS (Figure 5.3(b)) images show that workpiece adhesion (Fe element) and BUE occur during machining. The observation agrees with the literature review [13] that BUE has a high tendency to form during mild steel machining.

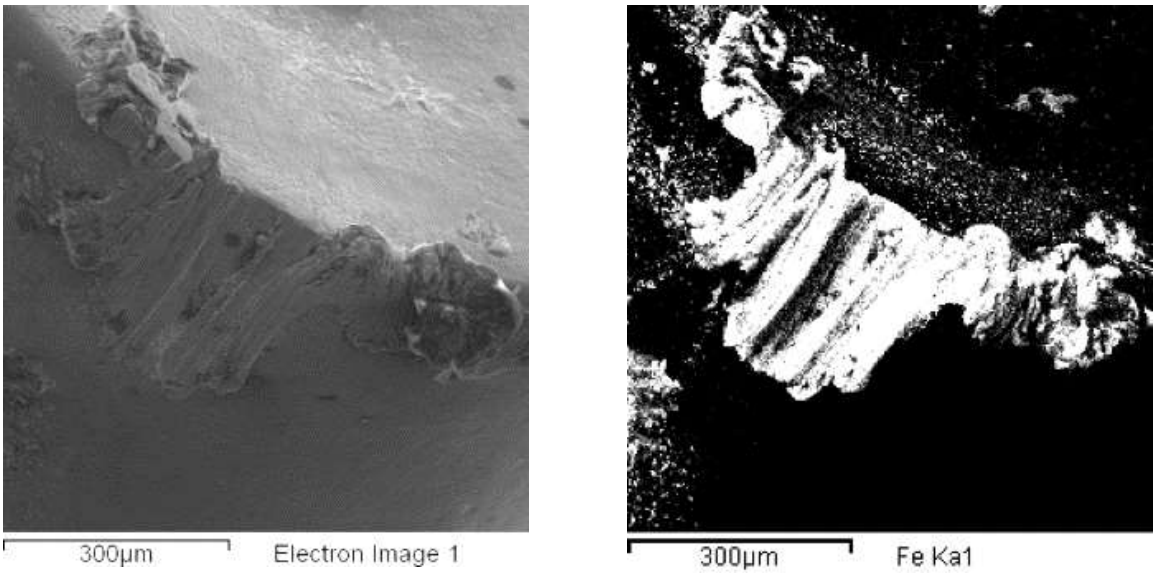

(a) (b)

Figure 5.3 (a)SEM, (b)EDS Fe distribution image of PVD Coated Carbide after 300 µm of Flank wear

The results below compare the dry and wet cutting conditions of the coated CBN tool C1. For C1, the tool life is 20 percent longer under the dry condition than wet condition at 500m/min. As indicated in Figure 5.1, tool life enters a longer and relatively more stable steady state under the dry cutting condition compared to the coated carbide tool in both dry and wet condition, and coated CBN in wet condition. Although flank wear is greater in the steady-state zone, the surface finish and overall tool life were not negatively affected. Figure 5.4 below showed that coating delamination occurred under the dry cutting condition. The wear mechanism was mainly abrasion in both dry and wet cutting conditions.

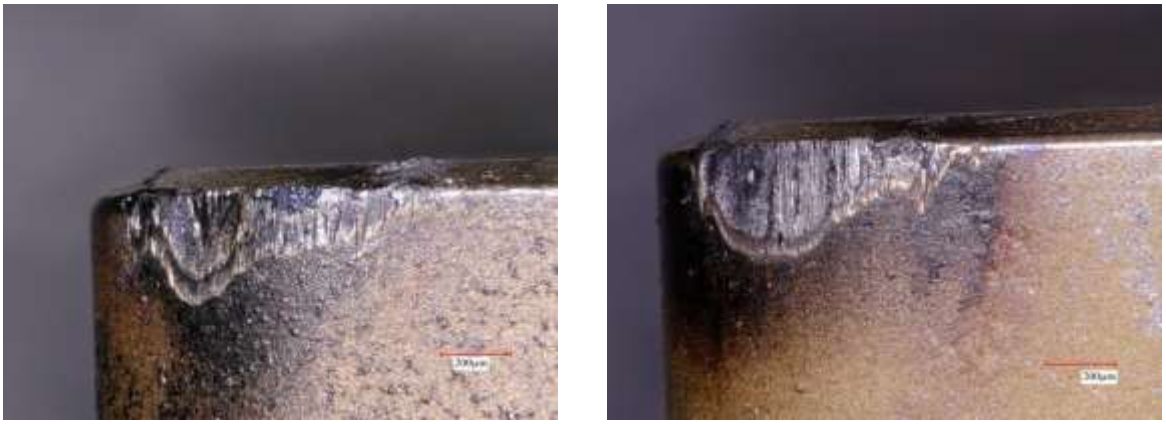

(a) (b)

Figure 5.4 C1 final flank wear before reaching 300-µm (a) Dry, (b) Wet Condition

Dry machining was selected as the preferable cutting mode for the rest of this study for CBN tools. From this study 5.1.1, dry machining shows no significant impact on tool life for coated carbide tool B0 and has an improvement in life for coated CBN tools. Dry machining also reduces coolant usage, making the manufacturing process more sustainable.

5.1.2 Effect of cutting speed on the performance of the uncoated CBN tool

The objective of this subchapter is to study the impact of cutting speed on uncoated CBN tool life during AISI 1018 machining.

According to the speed test plan, an uncoated CBN tool (U1) was selected to perform six tests under different surface speeds, with fixed feed rate and depth of cut. The results reveal the primary wear mechanism of the uncoated CBN during low carbon steel machining. An increase in cutting speed influences the tool life, surface integrity and machined part quality.

Figure 5.5 shows how tool wear intensifies with the increase of cutting speed. Each of the uncoated CBN tools maintains a constant wear rate throughout the entire tool life, without a steady-state of wear. This in accord with literature, where abrasion is reported to be the chief wear interaction of CBN with ferrous material. A cutting speed of 500 m/min was selected for the future tests since it falls into the high-speed region of LCS machining recorded in literature and features a relatively good tool life compared to even higher cutting speeds.

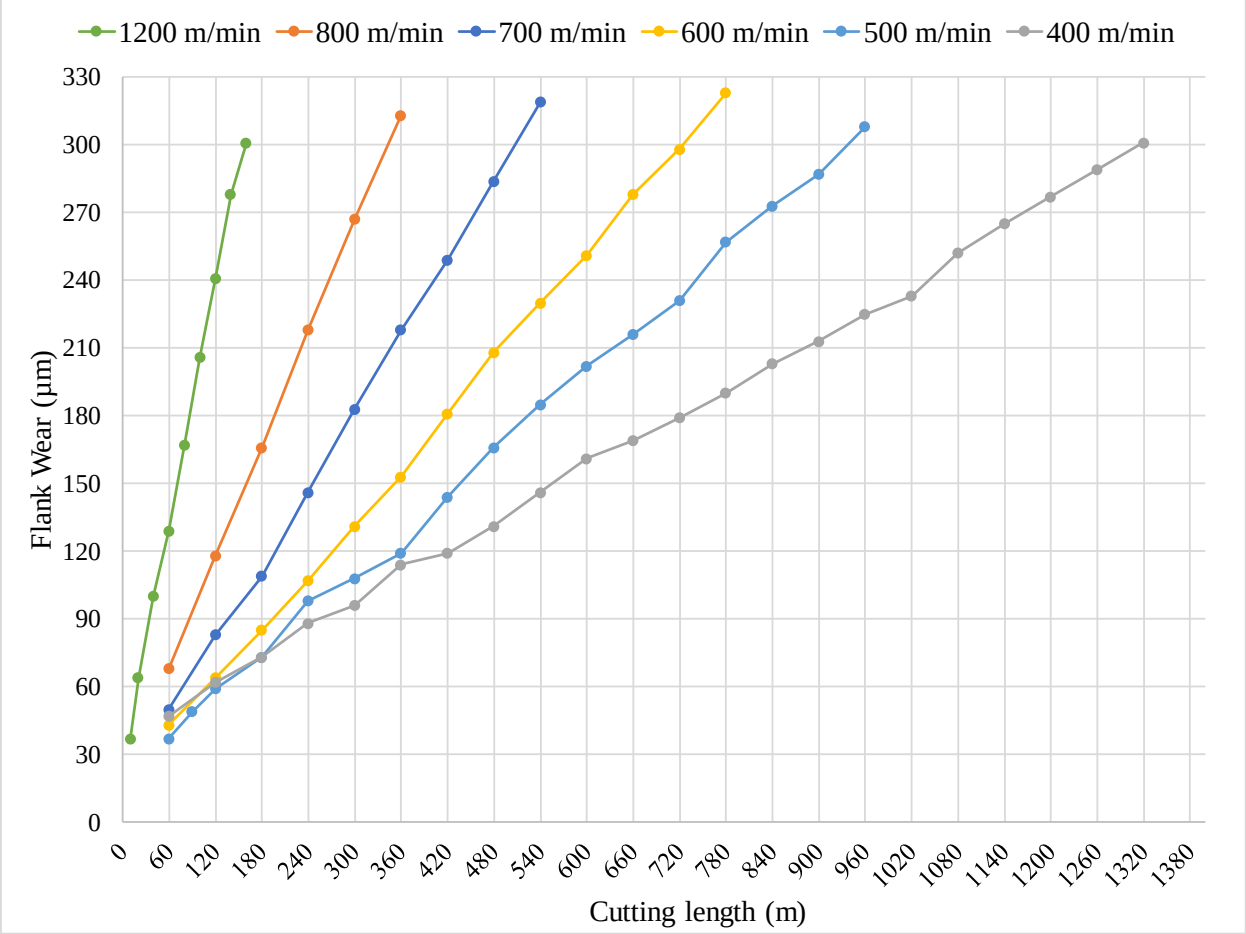

Figure 5.5 Wear vs. Cutting length curve of an uncoated CBN U1 tool under a dry condition

Figure 5.6 indicates that at a higher cutting speed, the abrasion wear on the flank face is more localized because of the decrease of the sticky zone at a high cutting load and temperature. As cutting speed decreased, the abrasion was distributed more uniformly on the flank wear zone.

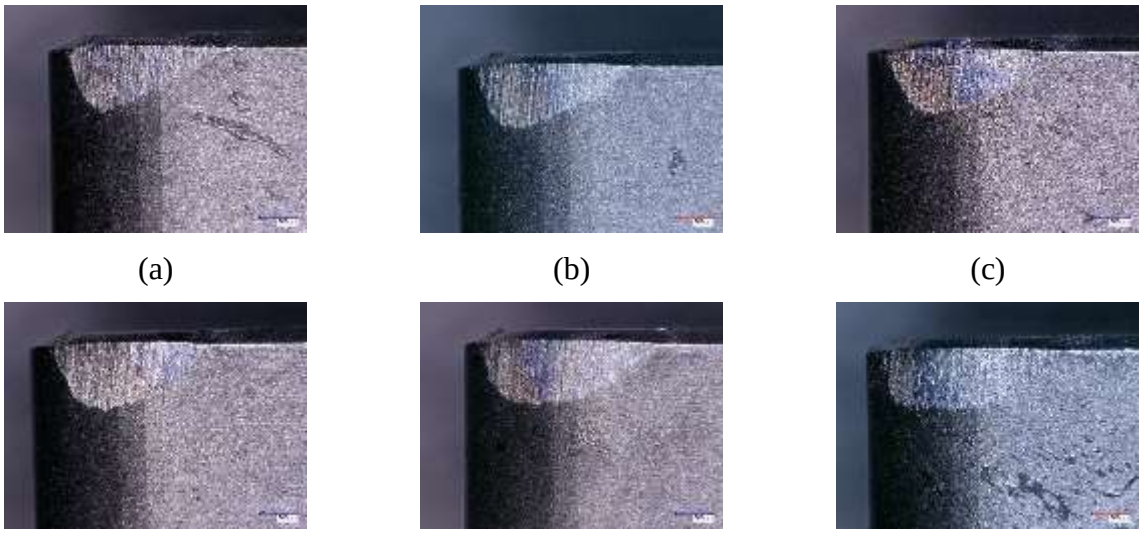

(a) (b) (c)

(d) (e) (f)

Figure 5.6 Speed test using U1 tool with Cutting speed of : (a)1200, (b)800, (c)700, (d)600, (e)500, (f)400 m/min

5.1.3 Summary

Further investigation of the wear mechanism is needed from the perspective of the substrate material, binder material and CBN grain size. More experiments at different cutting speeds and coating combinations could be carried out. Literature on CBN machining of hardened steels reports a similar conclusion to this study, that an increase in cutting speed increases the abrasion wear rate and reduces the tool life [40]. From this benchmark study, the dry cutting condition is chosen to be the cutting condition for the following studies. A cutting speed of 500m/min is selected for the remaining studies in this thesis to observe wear at a high cutting speed region.

5.2 Study A (Uncoated CBN tools)

The objective of Study A is to learn the effect of different CBN tool properties during LCS machining at a selected cutting speed. A focus is made on the tool life impact of the binder material, grain size and CBN content.

5.2.1 Tool Wear Comparison

In this study, turning tests were performed using five different uncoated CBN tools. The cutting conditions used are listed in the design of experiment Chapter 3, where the workpiece material is AISI 1018 low carbon steel. Tool flank wear was observed and measured using a Keyence VX5000 optical microscope after each selected cutting length. Corresponding tool flank wear curves for five uncoated CBN tools are shown in Figure 5.9.

Figure 5.7 below shows the tool life of five different uncoated CBN tools (U1-U5) and B0 for comparison. Tool wear curves vary with the composition of tool substrate materials. All uncoated CBN tools had a similar wear mechanism, but with different characteristics and properties, the tool performance varied in terms of tool life and wear rate.

The U1 tool has the shortest tool life among the five CBN cutting inserts. U2 and U4 tools have a similar tool wear trend and tool life. An obvious enhancement was found in the life of the U5 tool compared to the aforementioned three tools. U3 performed the best among all other selected uncoated CBN tools in terms of having the lowest tool flank wear rate and longest tool life. U3 also outperformed the tool life of the B0 benchmark carbide by 307% with better surface integrity.

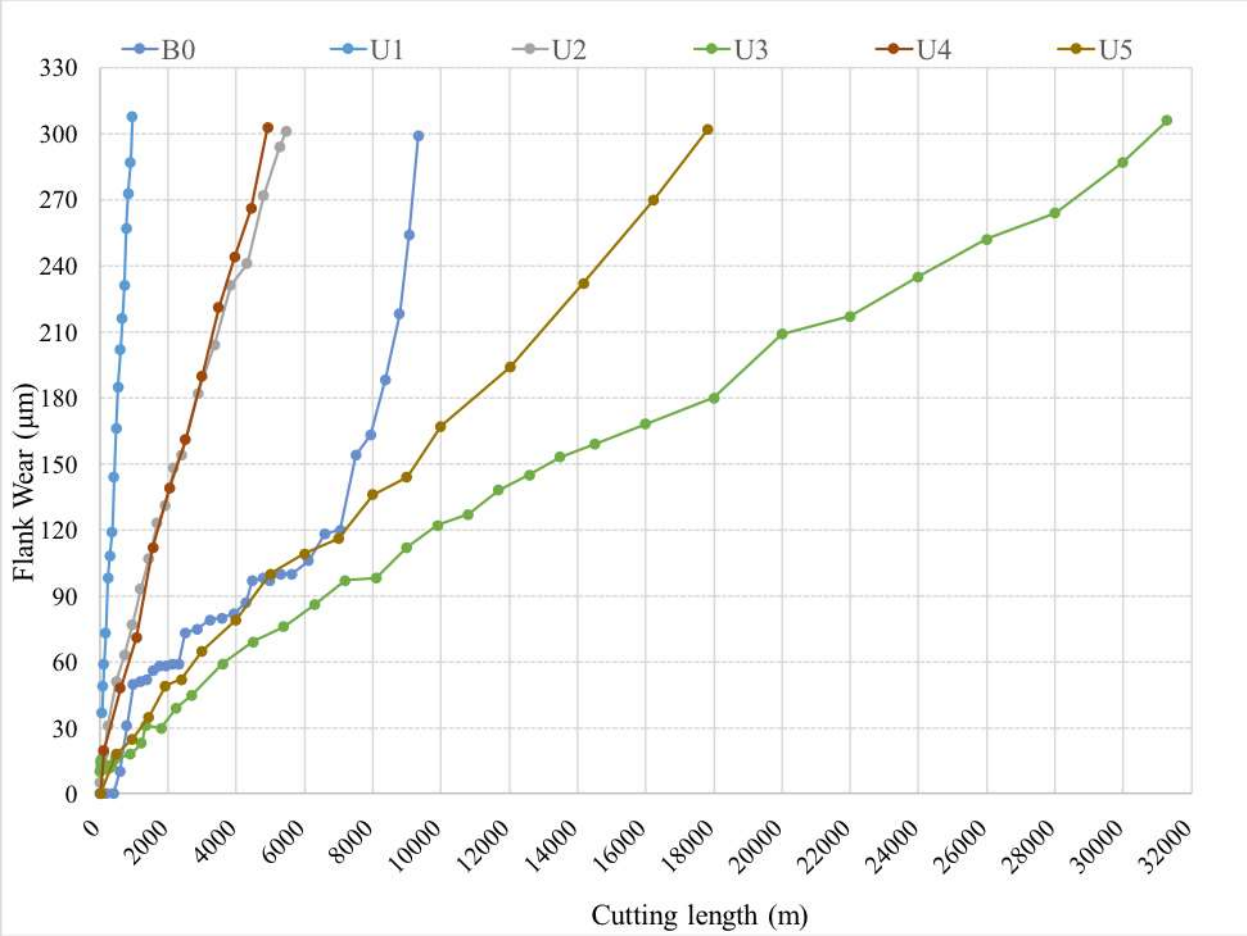

Figure 5.7 B0 and Uncoated CBN tools Wear vs. Cutting length

According to the tool property characterization results in Table 4.2 and the literature review, the major contributors to tool life extension are smaller CBN grain size, low CBN content, and binder material type. Huang et al. reported the wear resistance increases monotonically with decreasing CBN grain size during hard steel turning [40]. U2, U3, and U4 tools have a similar average grain size of 1µm, but their binder materials are different (U2: TiN U3: TiCN U4: TiN). It can be seen that the TiCN binder material contributes positively to the tool life because it helps slow the abrasion wear on the tool-workpiece interface.

U3 has the average substrate hardness of 4560 HV compared to other selected uncoated CBN tools (5103HV, 4009HV, 4476HV, 4640HV for U1, U2, U4, and U5 respectively). The performance of U3 indicates that TiCN is the preferred binder material for enhancing the strength and reliability of CBN tools during the cutting of AISI 1080 steel.

The U1 tool with 10 μm CBN grain size has an extremely short tool life. According to Sahin's work, for hardened steel machining low CBN containing tools consistently outperform tools with a high CBN content. The flank wear rates were proportional to cutting speed and high CBN tools exhibited accelerated thermal wear associated with high cutting temperatures [32]. For stainless steel and cast-iron machining using CBN tools with the same binder material and percentage content, wear rate intensifies along with the growth of grain size and cutting speed. The same trend applies to low carbon steel machining process using CBN tools.

Although U2, U4, and U5 have the same binder material, U5 featured a longer tool life as well as lower flank wear growth rate, due to its lower CBN content compared to U2 and U4. According to Thamizhmanii and Hasan's report, flank wear formation was mostly caused by abrasion [42].

Lower CBN content in ferrous material machining provides better abrasion wear resistance while retaining good hardness and heat resistance.

In summary, the U3 tool has the most preferable tool properties related to performance, which consist of low CBN content (40-45%), small grain size of 1μm and a suitable TiCN binder material.

5.2.2 Cutting Force Analysis

The average force data for the uncoated CBN tools are shown in Figure 5.8 below (U1 cutting force data was not collected, due to a technical barrier during the early stage of the experiment).

The force data were within a similar range. Since the geometry of the selected tools is similar, the cutting force is expected to also be similar. U3 has the longest tool life and the lowest average cutting force throughout the experiment. U5 was the second-best performing tool, with the second-lowest average cutting force shown in Figure 5.10. The geometry of U2 and U4 are not the same, but the average cutting forces and the performance in terms of tool life and tool wear were identical, as can be seen in Figure 5.7.

In summary, the results show that in the uncoated U1 to U5 CBN tools, a longer tool life corresponded to a smaller average cutting force. This indicates that the heat generated during the cutting process played a significant role.

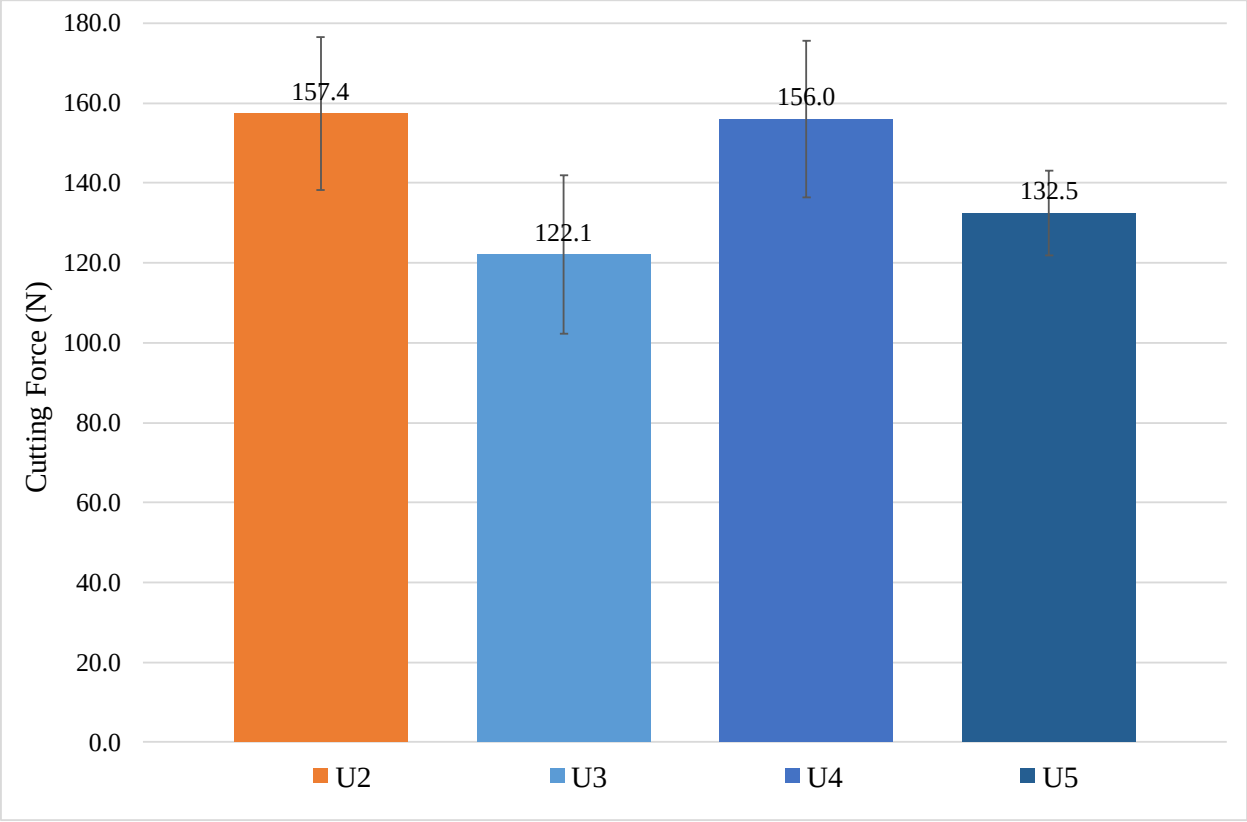

Figure 5.8 Average cutting force comparison of uncoated CBN tools

5.2.3 Wear Mechanism Analysis

A systematic analysis of the tool wear mechanism was made, which included tribofilm analysis and tool wear comparison after the failure of each tool (flank wear width reached 300 µm). Figure 5.9 shows that when the tool flank wear reached 300 µm, the shape of the abrasion wear area on the flank face remained almost the same. Abrasion texture was left on the flank face of each tool edge. Flank wear is the dominant wear type, followed by slight crater wear and oxidation wear on the boundary of the cutting area during the early stage of the cut.

(a) (b) (c) (d) (e)

Figure 5.9 Uncoated CBN (a)U1, (b)U2, (c)U3, (d)U4, (e)U5 Final Wear inspection. Cutting speed of 500 m/min, dry condition.

The SEI images in Figures 5.10, 5.11, 5.12, 5.13, and 5.14 show a clear abrasion mark on the flank face along with minor crater wear on the rake face. The crater wear is the worst in U3 since it has the longest tool life. More material is removed via the tool-workpiece interaction, leading to more wear on the rake face of U3. A possible cause for this is chip adhesion due to the high temperature present during the long tool life. Tool crater wear is not as severe as the flank wear on the flank face. Crater wear is caused only by abrasion between the flowing chip and the tool rake face, whereas flank wear is the product of thermal and high mechanical loads during the machining process.

Figure 5.10 below shows the EDS analysis results of the U1 tool. A large number of *Fe* particles is distributed on the flank face. This is one of the main reasons for the worst performance of U1 out of all the tested uncoated inserts. Very small amounts of *Mn* and *S* were found in the EDS images.

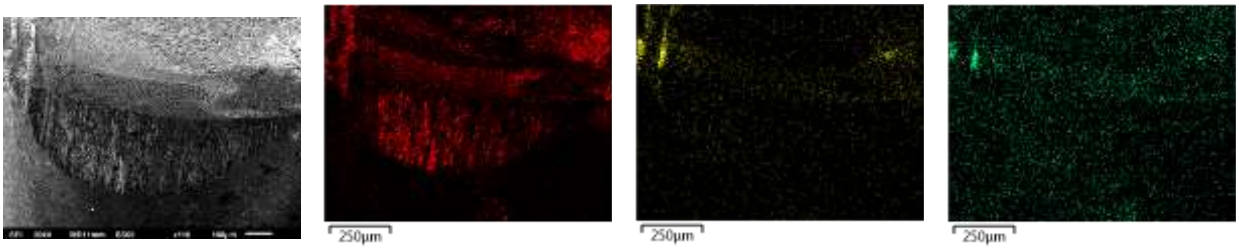

(a) (b) (c) (d)

Figure 5.10 U1 Wear inspection and EDS analysis performed in SEM: (a)SEI Image, Distribution of (b)Fe, (c)Mn, and (d)S element.

Figures 5.11 show the EDS analysis results for tool U2. *Fe* particles are distributed on the bottom flank face of the U2 tool. A large amount of *Mn* and *S* was found on the U2 and U3 flank faces, as can be seen in the EDS images.

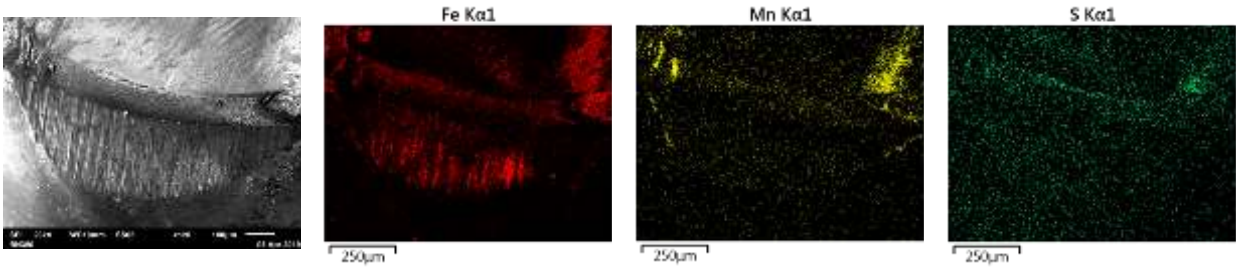

(a) (b) (c) (d)

Figure 5.11 U2 Wear inspection and EDS analysis performed in SEM: (a)SEI Image, Distribution of (b)Fe, (c)Mn, and (d)S.

Figures in 5.12 show the EDS analysis results for tool U3. A much smaller number of *Fe* particles was found of the U3 tool flank face, compared to tool U1 and U2. According to Yesong, a well balanced Mn and S manganese sulphide layer could help lubricate the cutting tool and improve machinability [7]. It can be seen from the EDS results that the U3 tool has low *Fe* adhesion at the flank face, and clear Mn boundary observed at the edge of cutting boundary.

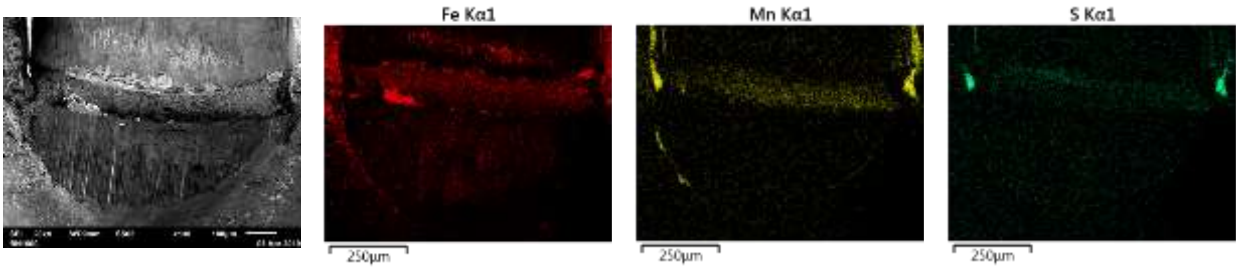

(a) (b) (c) (d)

Figure 5.12 U3 Wear inspection and EDS analysis performed in SEM: (a)SEI Image, Distribution of (b)Fe, (c)Mn, and (d)S.

Figure 5.13 shows that the *Fe* element distribution in the U4 tool is almost the same as that of U2, which remains constant throughout the tool life tests. Substrates U2 and U4 have a similar performance although they have different geometries (7.2-micron and 15.1-micron nose radius; bevel angle of 25.2 degree and 35.3 degree respectively) and CBN content (60-65% to 75% respectively), according to Table 4.1. The effect of decreasing in 10% CBN content is balanced by the effect of having 7.9-micron bigger nose radius and 10.1 degrees more in bevel angle.

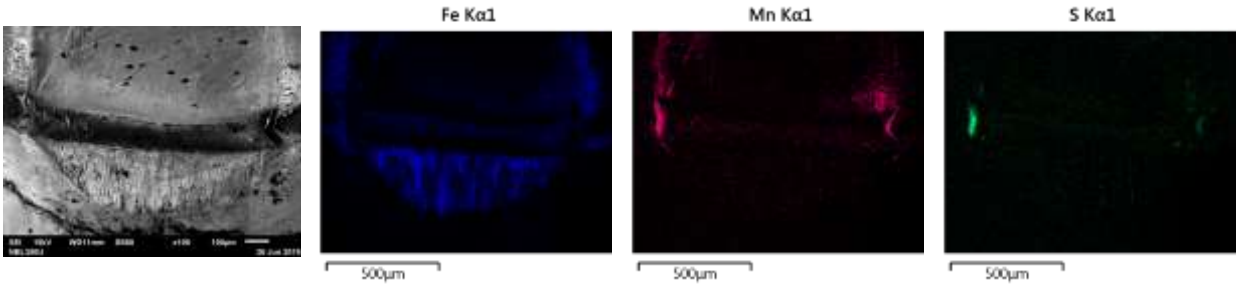

(a) (b) (c) (d)

Figure 5.13 U4 Wear inspection and EDS analysis performed in SEM: (a)SEI Image, Distribution of (b)Fe, (c)Mn, and (d)S.

Figure 5.14 shows the EDS analysis of the uncoated U5 CBN tool after machining. This tool has the second-longest tool life compared to the other uncoated CBN inserts. However, a large number of Fe particles can be seen in the EDS result, which is abnormal. Compared with U2 and U4, the U5 tool has around 10%-20% less CBN and a larger average grain size (U5: 2 µm; U2 and U4: 1 µm). Thus, not only does the Fe built-up edge influence the tool wear and tool failure, but a relatively lower CBN content and appropriate grain size also has a positive effect on tool performance.

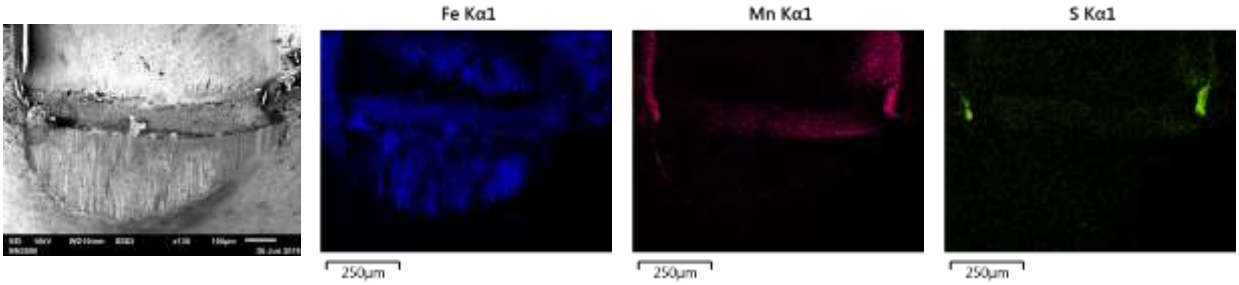

(a) (b) (c) (d)

Figure 5.14 U5 Wear inspection and EDS analysis performed in SEM: (a)SEI Image, Distribution of (b)Fe, (c)Mn, and (d)S.

5.2.4 Summary of Study A

Study A focuses on the performance of the uncoated CBN tools during the turning of AISI 1080 low carbon steel. Tool properties from Chapter 4 are compared with the test results from the experimental plan in Chapter 3. The data consist of the tool performance comparison, tool wear analysis with optical microscope and SEM and a series of EDS analyses. Based on the literature review and the characterization of the uncoated CBN materials, the properties of the substrates were linked with tool performance in this study. Grain size and the binder materials were found to play a significant role in tool life.

Significant findings in Study A:

1. The best performing tool, U3, had the lowest Fe content adhering to the flank face and has a tenfold longer tool life compared to the worst-performing U1 tool.

2. U1 has a greater average grain size (10 μm) than that of U2 and U3 (1 μm) and a higher CBN content, which reduces tool life and escalates flank wear. The grain size has a significant effect on the tool life differences between the tools. This result agrees with Oliveira et al. for CBN tools during the machining of hardened steels and cast iron [41].

3. U2 and U3 have different binder materials, respectively TiN and TiCN, which significantly affect the tool life.

During LCS dry cutting at 500 m/min, the major wear mechanisms of uncoated CBN tools were minor adhesion and early-stage oxidation. According to Huang et al., the CBN tool wear mechanism during the hard-turning process consists of abrasion, adhesion, and diffusion. In LCS

machining, the primary wear mechanism was abrasion, caused by CBN particles detached from the binder by the workpiece. CBN particles along the workpiece created abrasion marks along the flank face, according to previous findings[40]. This explains why the wear rate decreased with the same binder material and smaller grain size (refer to finding 2). The binder materials (TiCN, TiN, and WCo), each with their own chemical stability and properties, alter the wear rate by varying extents, which explains the performance differences between the tools (refer to finding 3).

To evaluate coating performance, each of the substrates in the next study will be compared to a coated CBN tool with a similar substrate (from Study A). The performance of the coating will be compared with that of the substrate reported in Study A.

5.3 Study B (Coated CBN tools)

The objective of Study B was to select the best performing coating suitable for CBN inserts to machine LCS at the selected cutting speed. The choice of coatings suitable for LCS machining are Al2O3, TiAlN, TiCN and AlTiN, with carbide tool B0 serving as the benchmark.

5.3.1 Tool Wear Comparison

Turning tests were performed on four coated CBN tools. The cutting conditions are specified in Study A and in Table 5.2, using the same workpiece material. Tool flank wear was observed and measured under an optical microscope after each selected cutting length.

Coated tools comparison:

Figure 5.15 below lists the tool life of all four different coated CBN tools (C1-C4) compared with B0. Each coated tool has a unique wear curve and performance at the testing condition.

The C4 tool has the shortest tool life among the four cutting inserts, and it is the only coated CBN tool that did not outperform the B0 benchmark coated carbide tool. C1 and C2 tools have a similar tool life but very different wear trend. An obvious enhancement was found in the life of the C3 tool compared to the aforementioned three tools. C3 performed the best among all other selected coated CBN tools in terms of having the lowest tool flank wear rate and longest tool life. C3 outperformed the tool life of the B0 by 241% with the same surface integrity.

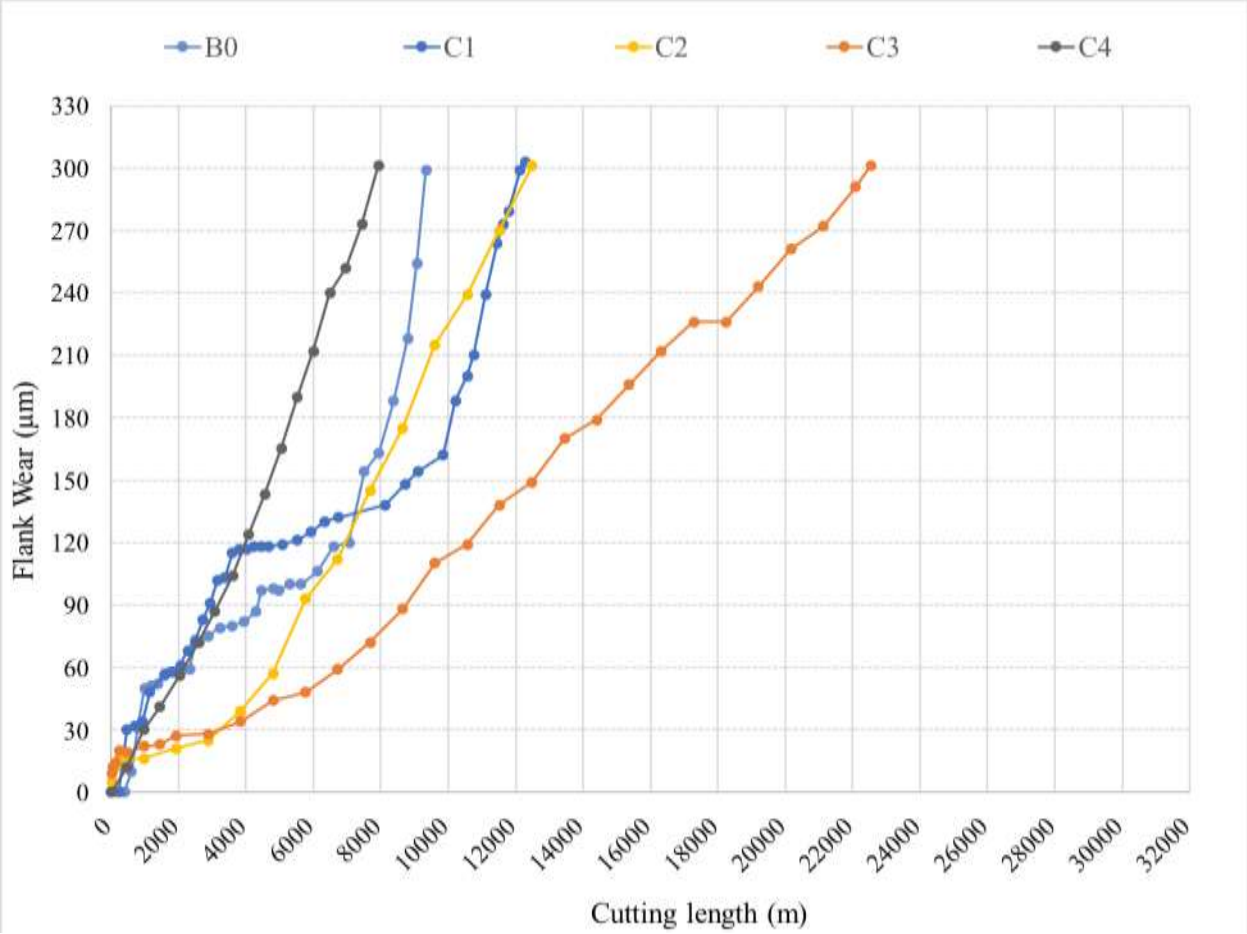

Figure 5.15 Coated CBN C1, C2, C3, C4 and Coated Carbide B0 Wear vs. Cutting length

Pair A (U1 vs. C1):

Figure 5.16 below shows the Coated CBN insert C1, which has a similar substrate material to U1. This coating material provided 11000 meters extra tool life to the substrate. According to Table 4.2, both tools have a grain size of 10 µm, which is relatively big compared to the other pairs of inserts. The U1 has the shortest tool life in Study A. However, the coating material offers good protection against wear. According to Naskar et al., the CVD Al2O3 coating is suited for low carbon steel machining [4].

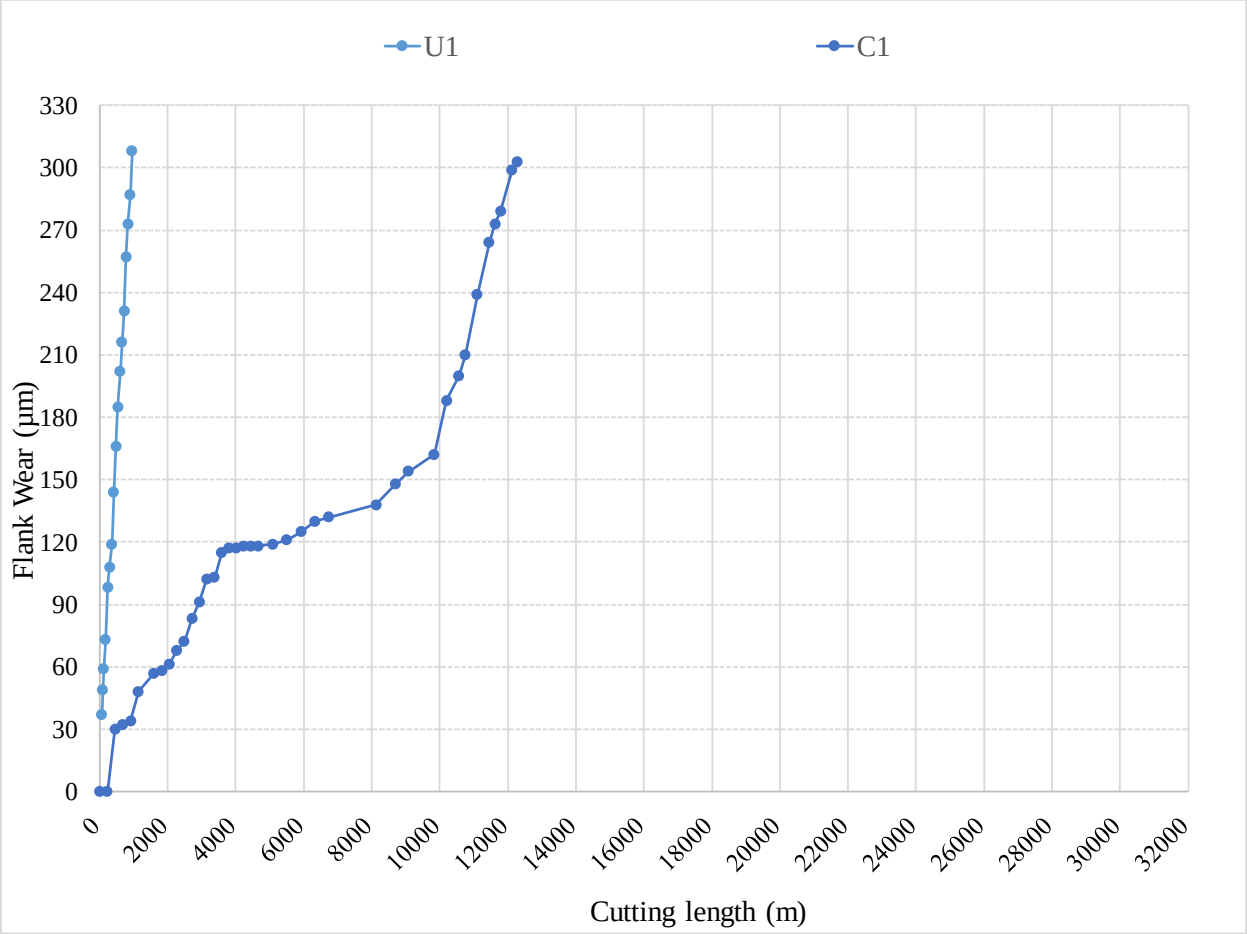

Figure 5.16 Coated and Uncoated CBN Pair A, U1&C1 Wear vs. Cutting length

Pair B (U2 vs. C2):

Figure 5.17 below shows the C2 performance. C2 has a similar substrate material to U2. The coating material was PVD deposited TiAlN. The substrate of this pair of CBN tools has the most similar composition to the other two pairs. The TiAlN coating extended the substrate's tool life by an extra 7000 meters. According to Naskar et al., the TiAlN PVD coating is also applicable for machining low carbon steel. At 600m/min for the same substrate, it has comparable flank wear to the Al2O3 coating, which is less than that of the TiCN PVD coating [4].

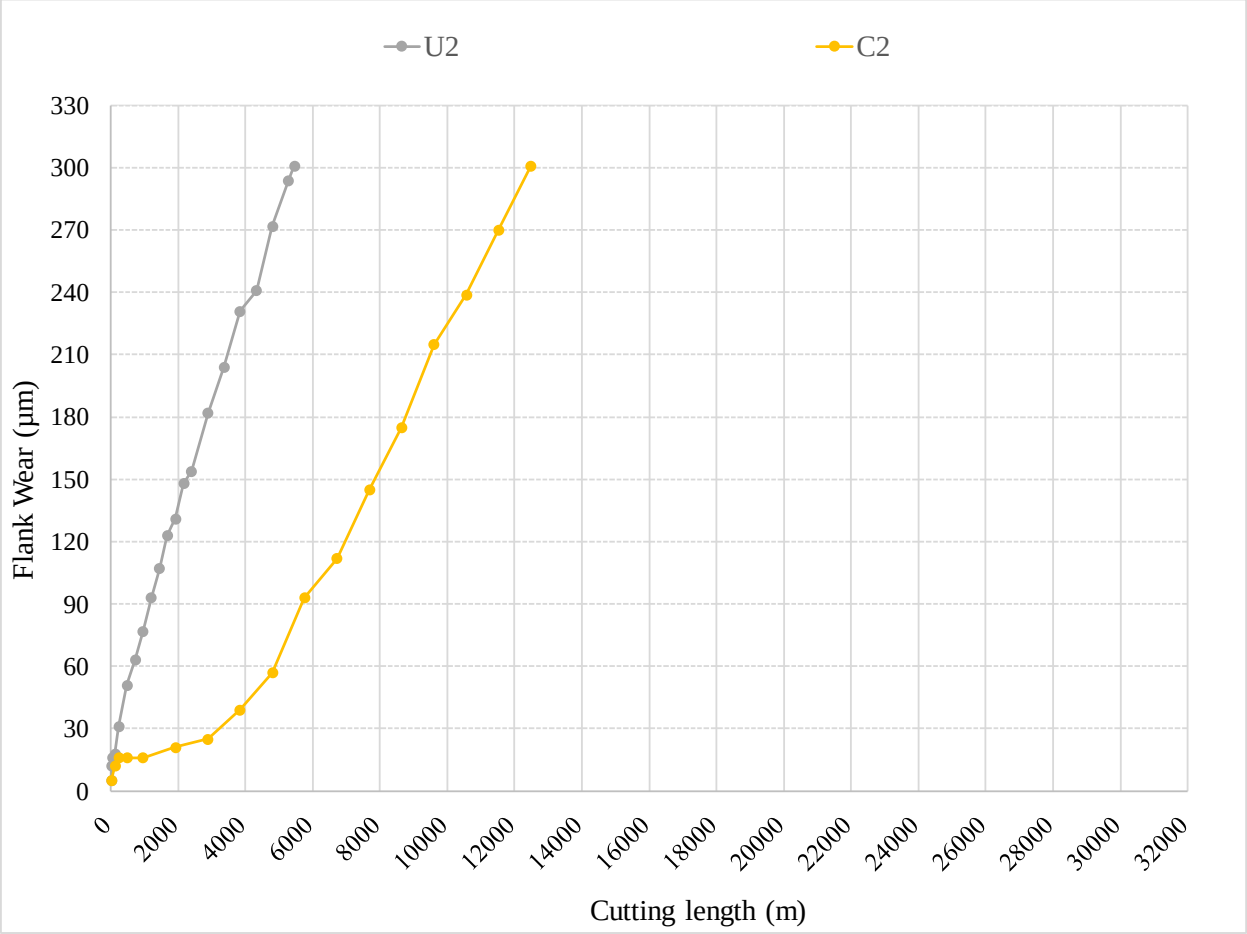

Figure 5.17 Coated and Uncoated CBN Pair B U2&C2 Wear vs. Cutting length

Pair C (U3 vs. C3):

Figure 5.18 below compares the tool life of the coated C3 CBN insert to that of the uncoated U3 insert. Both tools have the same TiCN binder material and high CBN content. The reason the uncoated tool outperformed the coated tool could be that the grain sizes are 1-micron and 2-micron for uncoated and coated tools, respectively. A smaller grain size usually results in a longer tool life. Also, from SEM images, it can be seen that the coated tool C3 has a large number of porous defects in the substrate, whereas the uncoated U3 tools are more uniform. Finally, the coating may

increase the abrasion wear rate since the carbon present in it may form carbide particles during the machining process (under high temperature and pressure). Naskar et al. reported that out of the Al2O3, TiAlN, and TiCN coatings, TiCN coating performs the poorest in terms of flank wear resistance [4].

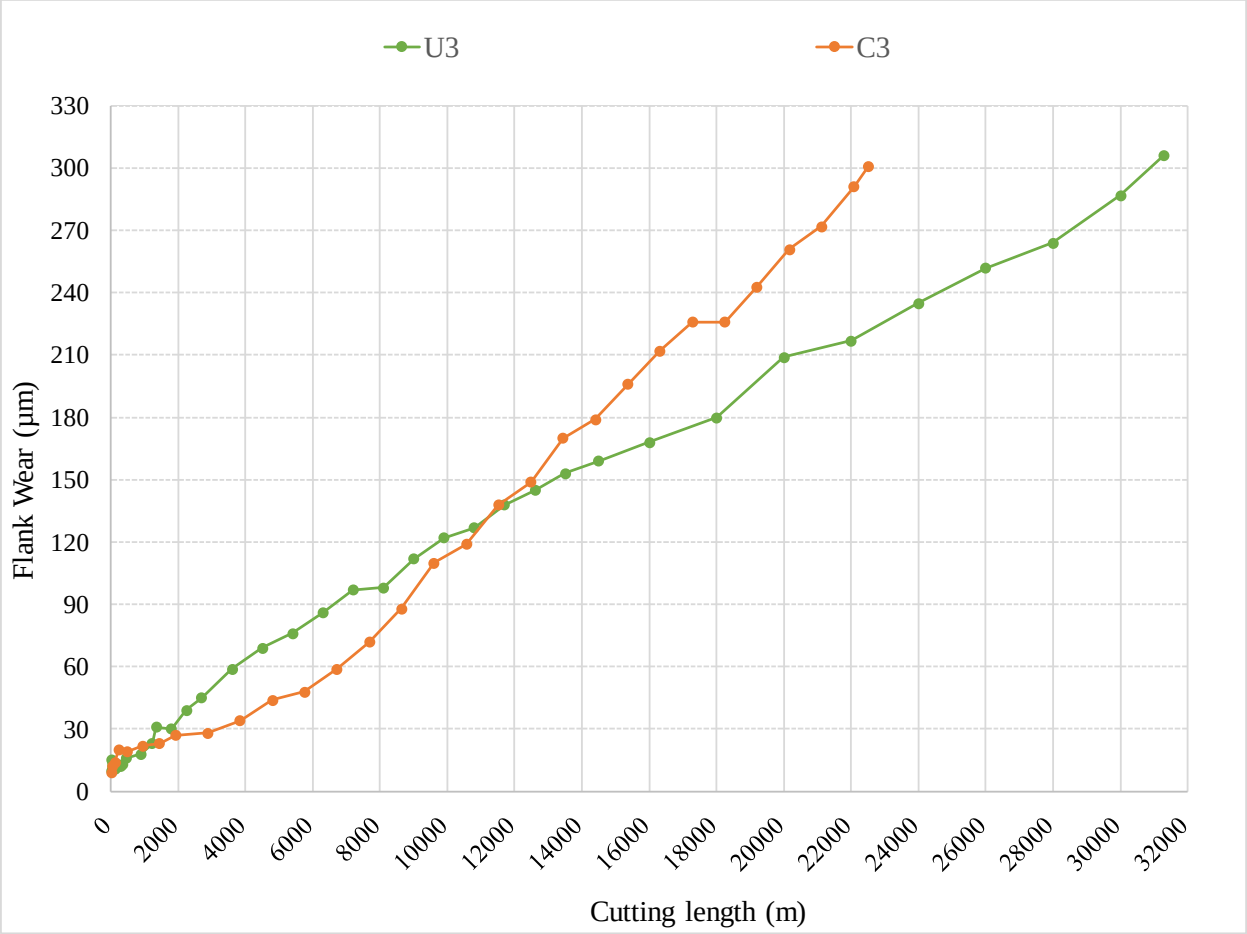

Figure 5.18 Coated and Uncoated CBN Pair C U3&C3 Wear vs. Cutting length

Pair D (U4 vs. C4):

Figure 5.19 shows the coated CBN insert C4, which has the same substrate material as U4. The coating is PVD AlTiN. The substrate of this pair of CBN tools has the closest composition to the U2 and C2. This AlTiN coating added 3000 meters of extra tool life to the substrate. Since U2 and U4 are similar in terms of tool substrate performance, it can be concluded that TiAlN performed better than AlTiN during a finishing operation on LCS at 500m/min.

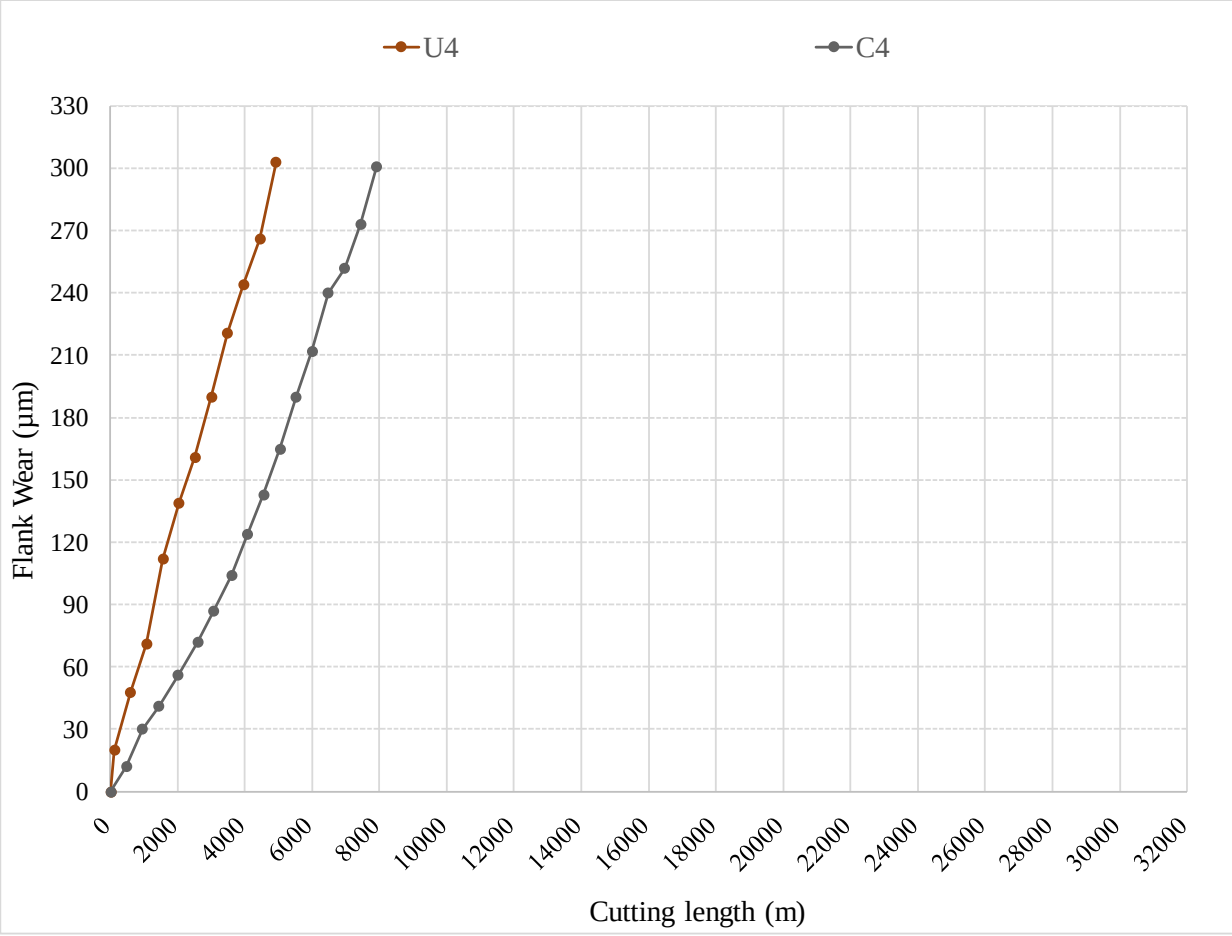

Figure 5.19 Coated and Uncoated CBN Pair D U4&C4 Wear vs. Cutting length

5.3.2 Cutting Force Analysis

The average force data for Coated CBN tools is shown in Figure 5.20 below (C1 cutting force data were not collected due to the technical barriers at the early stage of the experiment).

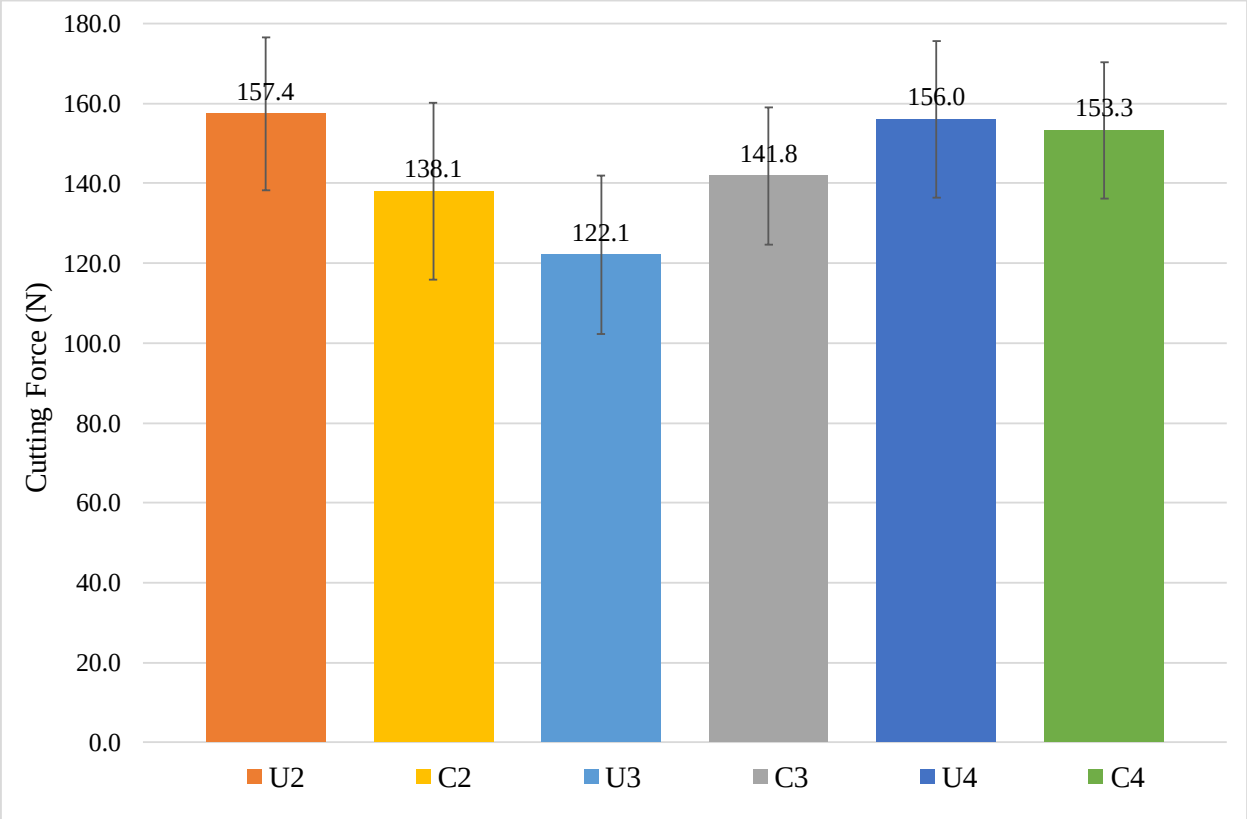

Figure 5.20 Average cutting force comparison for coated and uncoated CBN tools

Figure 5.20 above showcases the differences in the average cutting forces of different coated tools. Comparing the average cutting forces of coated and uncoated tools, it can be concluded that different coatings provide different lubricating properties and substrate protection. The average force in C2 significantly drops compared to U2, leading to a prolonged tool life, according to Figure 5.17. C4 has the shortest tool life and the highest cutting force. Although its average cutting

force is less than that of U4, this difference is less than 10%. In Figure 5.19, it can be seen that the AlTiN coating did not improve tool life as much as the TiAlN coated C2 tool. Although C3 has the longest tool life, the cutting force is greater than that of U3. Figure 5.18 shows that C3 has a shorter tool life compared to U3 and an accordingly greater cutting force. This shows the coating reduces the friction at the tool and workpiece interface, but does not reduce the wear resistance.

5.3.3 Wear Mechanism Analysis

Figure 5.21 below shows that when the tool flank wear reached 300 µm, the shape of the abrasion wear area on the flank face was different in each coated tool, depending on the wear mechanism. Clear coating delamination is observed in the C1 tool which has the thickest CVD deposited Al2O3 coating. Coating delamination also occurs at the end of tool life in C2, which has a PVD TiAlN coating. C3 and C4 did not feature the coating delamination boundary. The improvement of tool life achieved by C3 and C4 coatings was not obvious in Figure 5.19 and 5.20. Abrasion texture was left on the flank face of each tool edge. Flank wear is the dominant wear type, followed by slight crater wear and oxidation mostly at the boundary of the cutting area during the early stage of cut, as in study A.

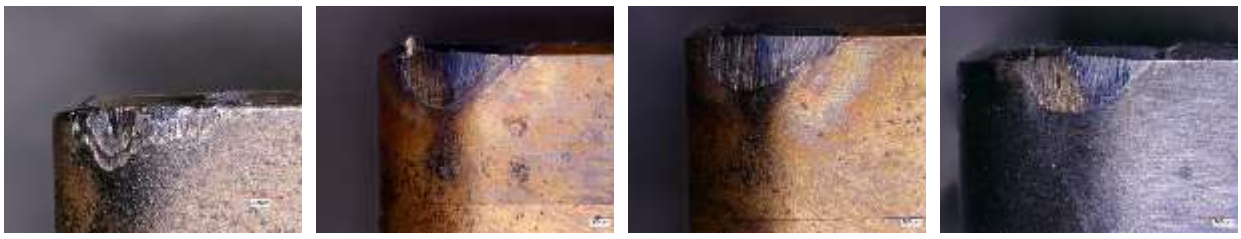

(a) (b) (c) (d)

Figure 5.21 Uncoated CBN (a)C1, (b)C2, (c)C3, (d)C4 Final Wear inspection

Cutting speed of 500 m/min, dry condition.

As can be seen in Figure 5.22, the coating material is alumina with a TiN outer layer. Adhesion of the Fe element at the end of tool life occurred in the form of BUE. Slight amounts of Mn accumulated on the edge of the rake face. No Mn-S was found in the EDS analysis.

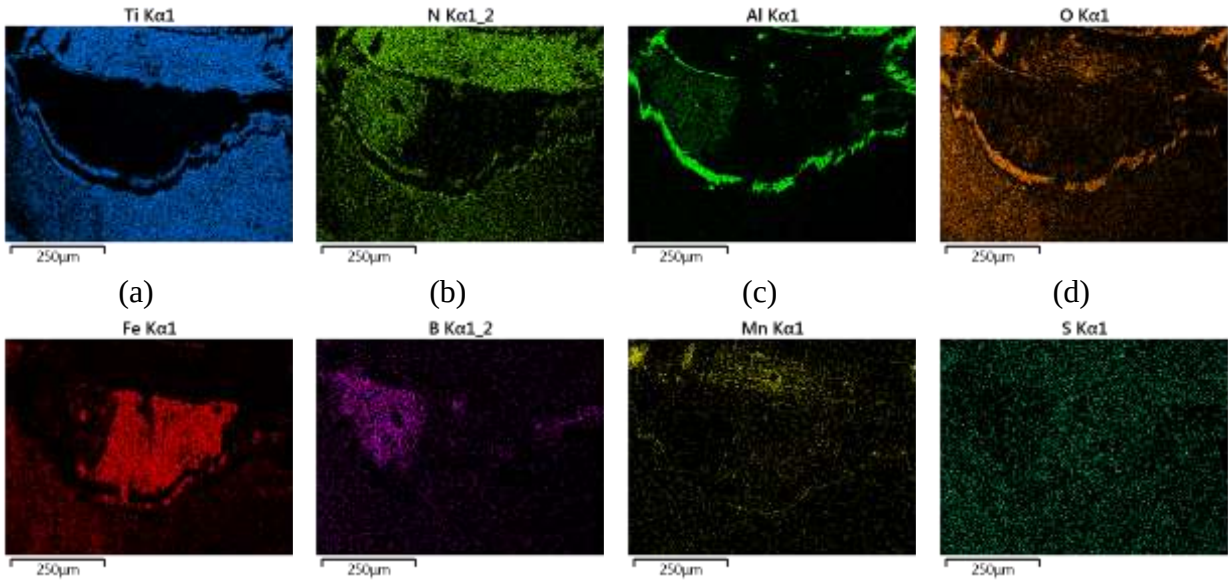

Figure 5.22 C1 Wear inspection and EDS analysis performed in SEM: Distribution of (a)Ti, (b)N, (c)Al, (d)O, (e)Fe, (f) B, (g)Mn, and (h)S.

Figure 5.23 shows less Fe adhesion on the C2 tool in comparison with C1, as well as the presence of Mn-S. As can be seen in Figure 5.24, a greater amount of Fe adheres to the C3 tool, which reduces the tool's life compared to U3. Mn-S was present at the end of the tool's life.

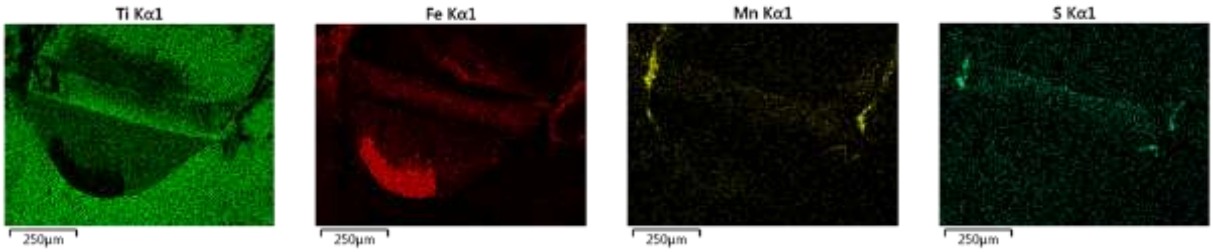

(a) (b) (c) (d)

Figure 5.23 C2 Wear inspection and EDS analysis performed in SEM: (a)SEI Image, Distribution of (b)Fe, (c)Mn, and (d)S.

Figure 5.24 large amount of Mn and S was present on the edge of the worn flank and rake face. Fe was evenly distributed at the flank face and rake face. Ti at the flank face and no sign of boron show the coating is intact with the substrate.

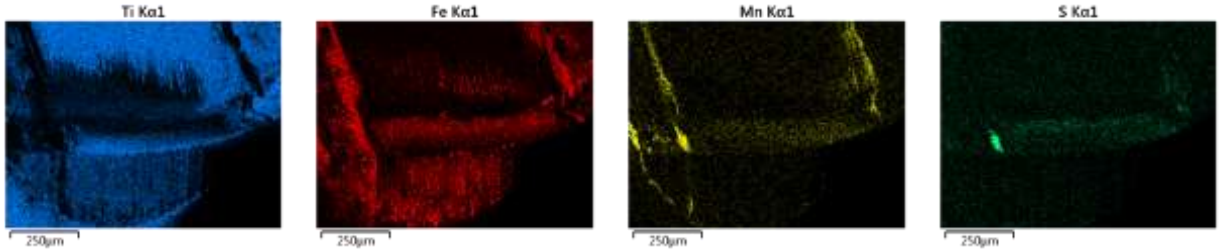

(a) (b) (c) (d)

Figure 5.24 C3 Wear inspection and EDS analysis performed in SEM: (a)SEI Image, Distribution of (b)Fe, (c)Mn, and (d)S.

A large amount of Fe was present on the flank face in figure 5.25, in the form of BUE concentrated at the bottom of the flank wear wedge. Mn and S was present on the edge of the worn flank and rake faces. EDS showed that the coating was composed of Al, Ti, N, which corresponds to the manufacturing data.

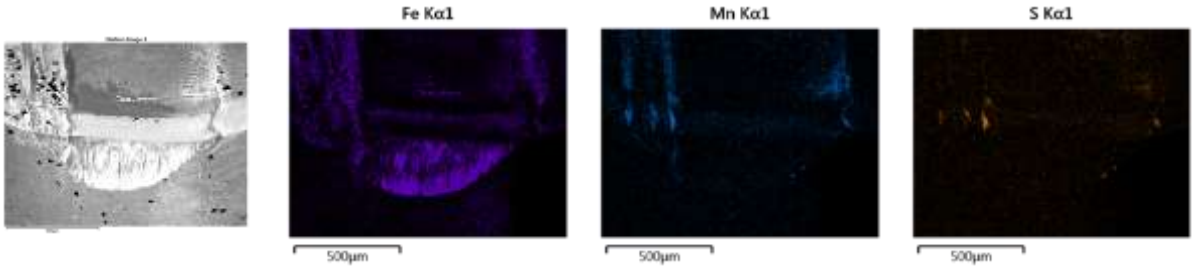

(a) (b) (c) (d)

Figure 5.25 C4 Wear inspection and EDS analysis performed in SEM: (a)SEI Image, Distribution of (b)Fe, (c)Mn, and (d)S.

5.3.4 Summary of Study B

Study B focused on the performance of the coated tools compared to an uncoated CBN tool with similar substrate content.

1. It was concluded that Al2O3 and TiAlN coatings offer better lubrication and extend tool life of CBN tools that have TiN as binder materials. The TiCN binder was found to provide great performance in combination with an uncoated tool (refer to Study A). The AlTiN coating did not perform as well as other coatings in terms of prolonging tool life. Application of a TiCN coating dramatically decreased the tool life (C3 vs. U3). The result agrees with Naskar and Chattopadhyay's study that evaluated the performance of Al2O3 and TiAlN coatings during LCS machining under a high-speed condition [4].

2. From the EDS result, all coated CBN tools did not have substrate exposed except C1. C1, C2 and C4 coatings prolong the tool life of their substrates by different amounts. Further investigation could be made for C3, as the coating reduces the cutting force during the machining process but shortened the tool life.

The next investigation will be made from first selection of substrate from Study A and selection of the best performing coating (CVD Al2O3 or PVD TiAlN) from Study B to form a new coated CBN tool for the test.

5.4 MMRI Coating for CBN Tool

The final Study selects a coating from Study B to be applied on the best performing tool from Study A. The goal is to achieve a combination of good CBN substrate and a suitable coating for low carbon steel machining.

Both Al2O3 CVD and TiAlN PVD coatings are suitable in terms of prolonging tool life for CBN tools with TiN binder during the dry machining of AISI 1018 at 500m/min (from U1 vs. C1 and U2 vs C2). This last study is to apply the selected coating on a different substrate (U1 and U3) to further study the coating behaviour. Due to its greater accessibility, only the PVD coating technique is available as of now. The TiAlN coating was applied on U1 and U3, which are respectively the worst and the best performing uncoated CBN tools. The C1 pair in Study B had a CVD Al2O3 coating. The performance of Al2O3 and TiAlN could be compared by applying a TiAlN coating on U1. U3 was the best uncoated CBN performer, but the C3 coating reduced performance of this good substrate. Applying the TiAlN coating to U3 will test the coating behaviour for TiCN binder CBN tool U3.

5.4.1 Tool Wear Comparison

Figure 5.26 below shows a comparison of U1 and C1 with an applied CU1 coating. The CU1 coating provides around 9000 meters extra tool life to the substrate. The C1 is still the best

performing coating, as it provides 11000 meters extra tool life to the substrate. CVD Al2O3 is a thicker coating compared to the PVD TiAlN coating. The Al2O3 CVD coating has better abrasion resistance and thermal barrier due to its high thickness. In cases when PVD coating application is simpler, cheaper and thinner, it can deliver better machining accuracy and tolerance grade to finished parts. [36]

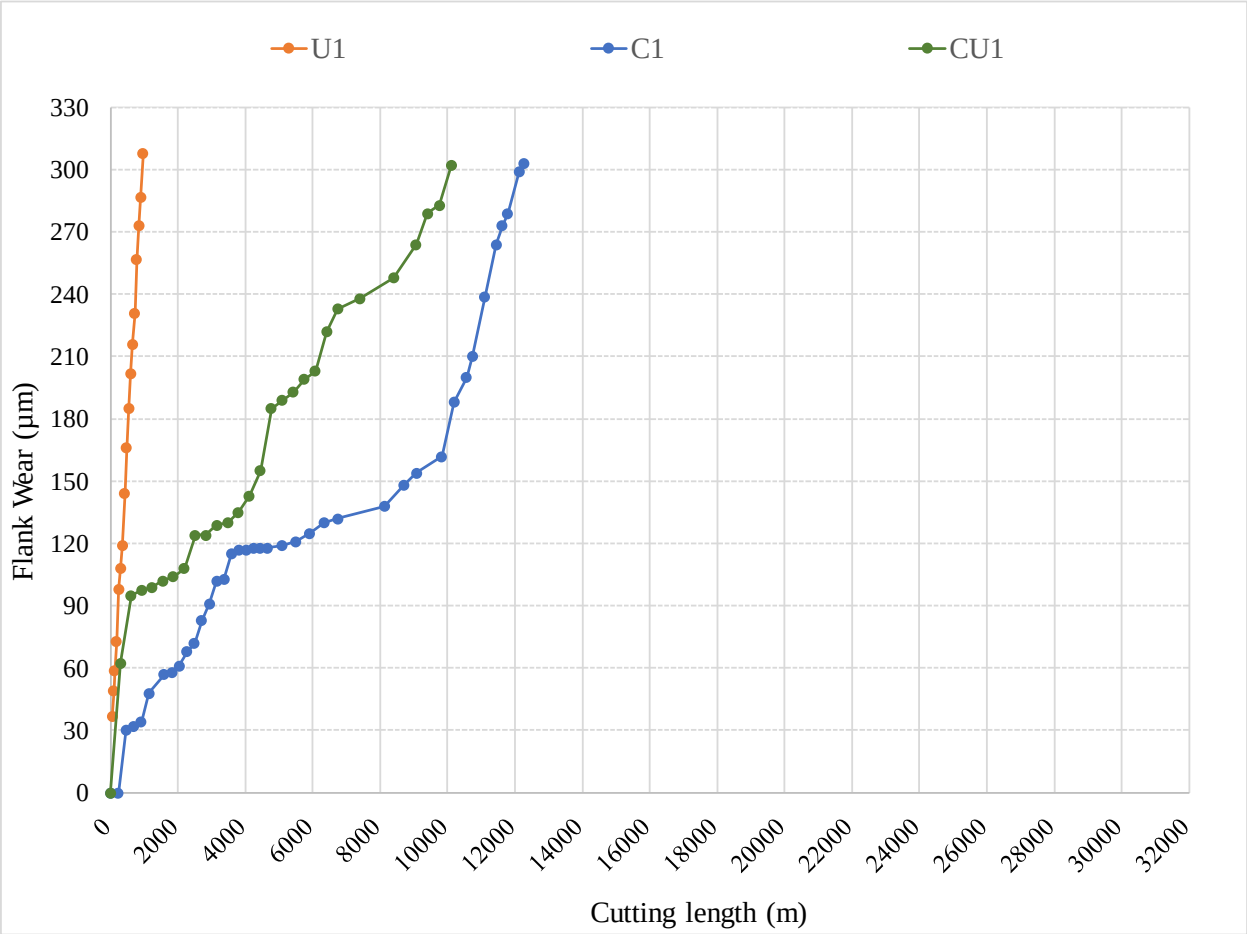

Figure 5.26 U1, C1, and CU1 Wear vs. Cutting length

Figure 5.27 below shows the tool wear curve comparison of U3, C3, and TiAlN coated U3. This coating reduced tool life, like U3 and C3. The results showed that the CBN tool with a TiCN binder

performed better when uncoated. Aizawa et al. [55] reported that the TiCN material could form a tribo-layer of TiOx, SiO2 and MnO at 400m/min Vc which would protect the cutting interface and increase the overall tool life of the substrate. Refer to Study A figure 5.12, the Mn and Si concentration shown in the SEM figures. Further investigation needs to be done to validate the tribofilm formation on TiCN binder CBN tools.

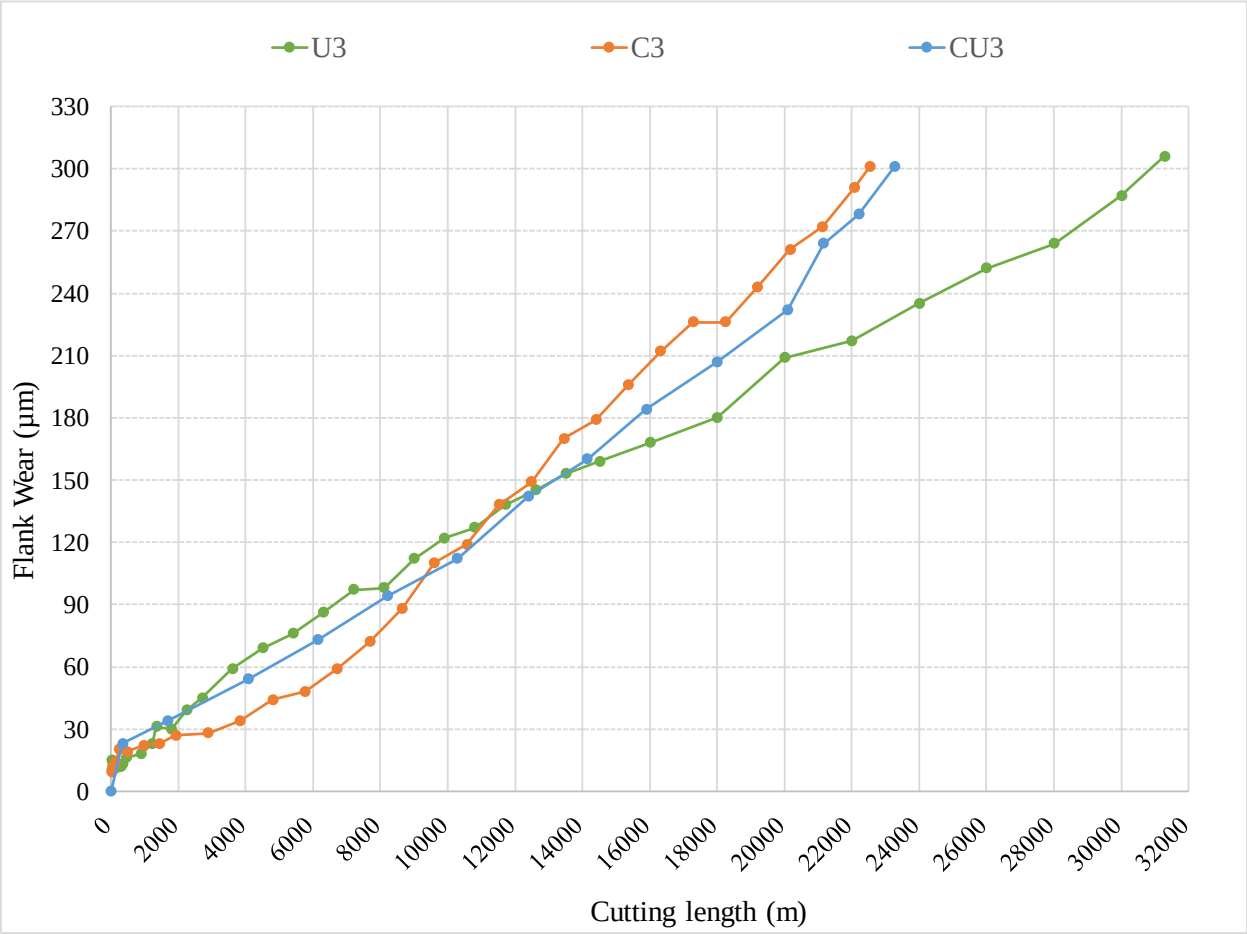

Figure 5.27 U3, C3, and CU3 Wear vs. Cutting length

5.4.2 Cutting Force Analysis

The average force data for the MMRI coated CBN tools are shown in Figure 5.28. The average cutting forces were reduced after the coating was applied. However, the cutting force reduction does not correlate with prolonged tool life in U3 and CU3. Further analysis below shows that although the coating provides better lubricity, the interaction between the substrate material and the workpiece shortened the tool life of U3.

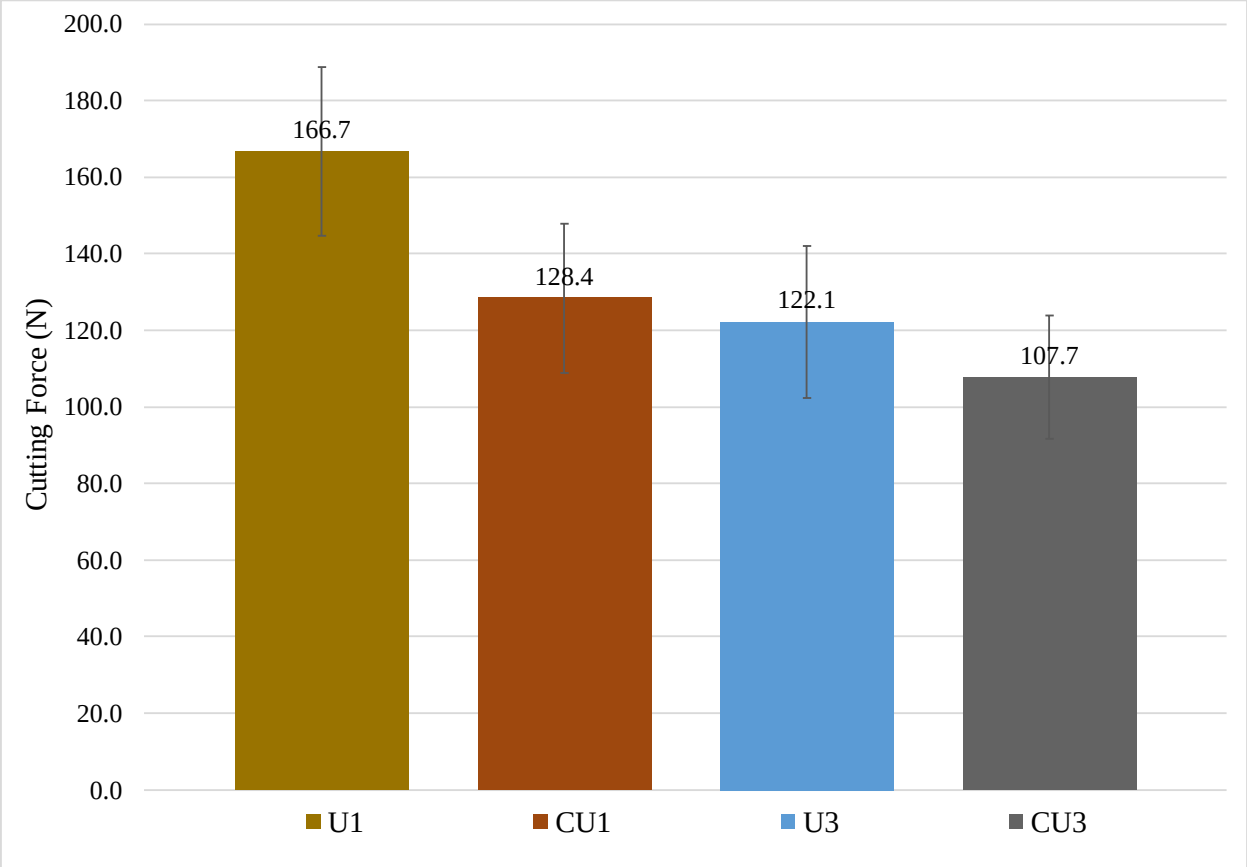

Figure 5.28 U1, U3, CU1, CU3 Wear vs. Cutting length

5.4.3 Wear Mechanism Analysis

The flank wear at the end of the 300-micron failure criterion is reviewed in Figure 5.29. It can be seen that CU1 had a deeper abrasion marks compared with CU3. The abrasion marks on the flank face of CU3 were more uniform. CU3 has better tool life than CU1.

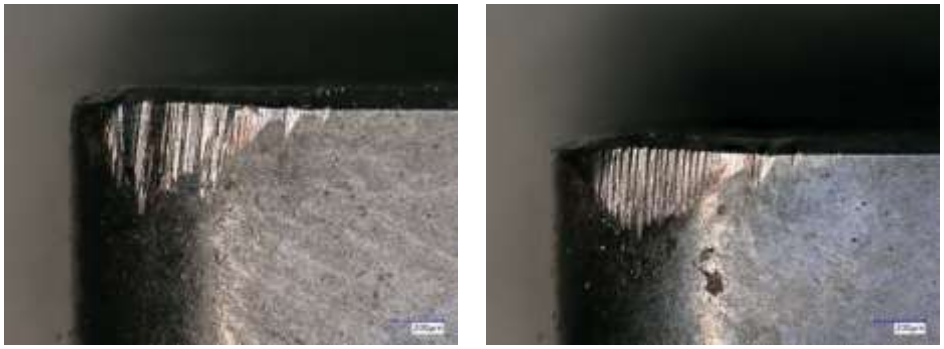

(a) (b)

Figure 5.29 *Uncoated CBN (a)CU1, (b)CU3 Final Wear inspection at a 500 m/min cutting speed and dry condition.*

Figure 5.30 below shows the EDS result for the CU1 tool at the end of the 300-micron flank wear test. The elements are shown correspondingly. The presence of Mn (f) at the cutting interface could be a sign of MnO formation. The missing titanium region in Figure 5.31 (c) and the exposed substrate material show that the coating is worn out at the flank face location.

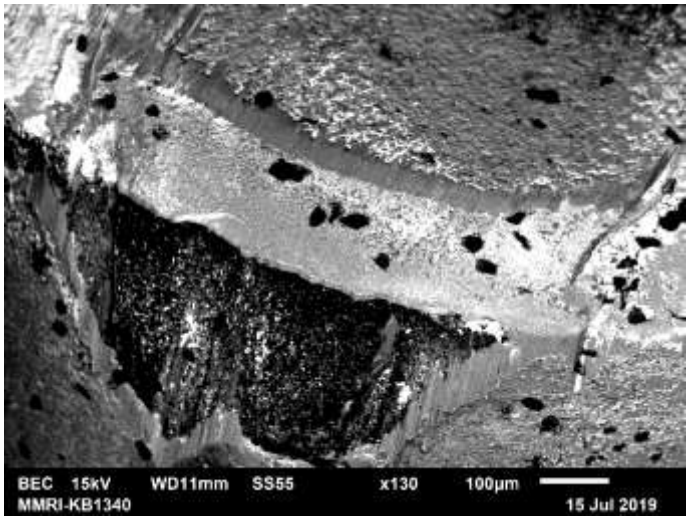

(a)

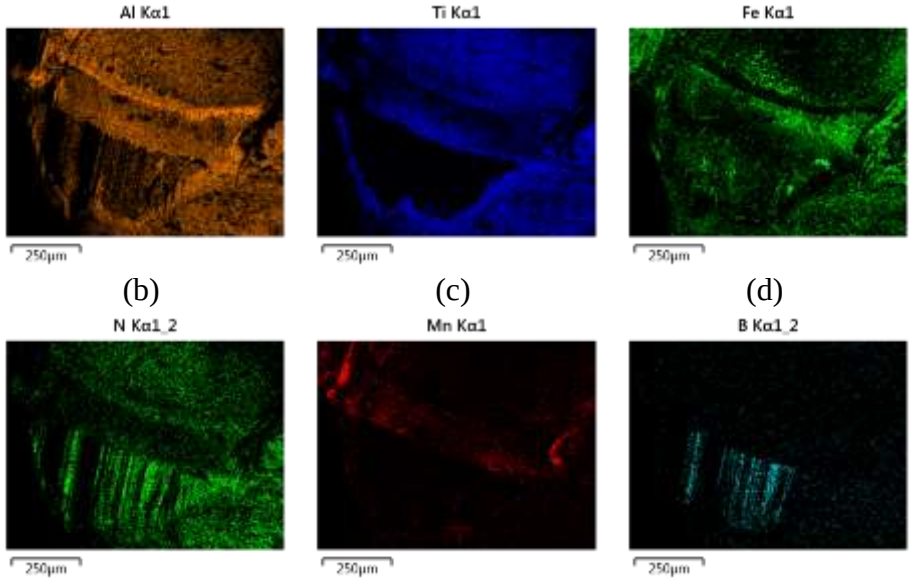

(b) (c) (d)

(e) (f) (g)

Figure 5.30 CU1 Wear inspection and EDS analysis performed in SEM: (a) BEC image and the distribution of (a)Ti, (b)Al, (c)Ti, (d)Fe, (e)N, (f) Mn, and (g)B element.

Figure 5.31 shows the EDS result of the CU3 tool at the end of a 300-micron flank wear test. The corresponding elements are listed. A large amount of Mn-S was found at the cutting interface. The Boron element was not detected in Figure 5.31 (h) and coating materials such as (b) aluminum and (c) titanium were found at the flank wear region, which means that the substrate material was not

yet exposed. The images show that the tool coating remained intact at the end of tool life, which prevents the substrate from being exposed to the workpiece material. Coating delamination did not occur in the CU3 coated tool. However, the tool life curve showed that the uncoated tool has better tool life, suggesting that interaction occurs between the U3 uncoated tool with the workpiece material during machining. This wear mechanism warrants further investigation.

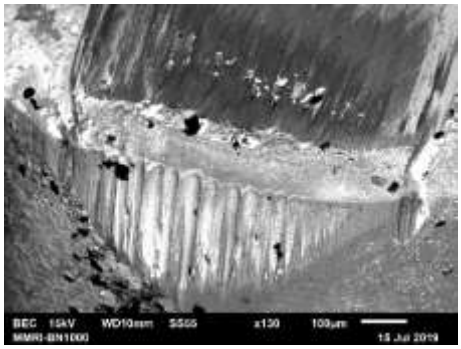

(a)

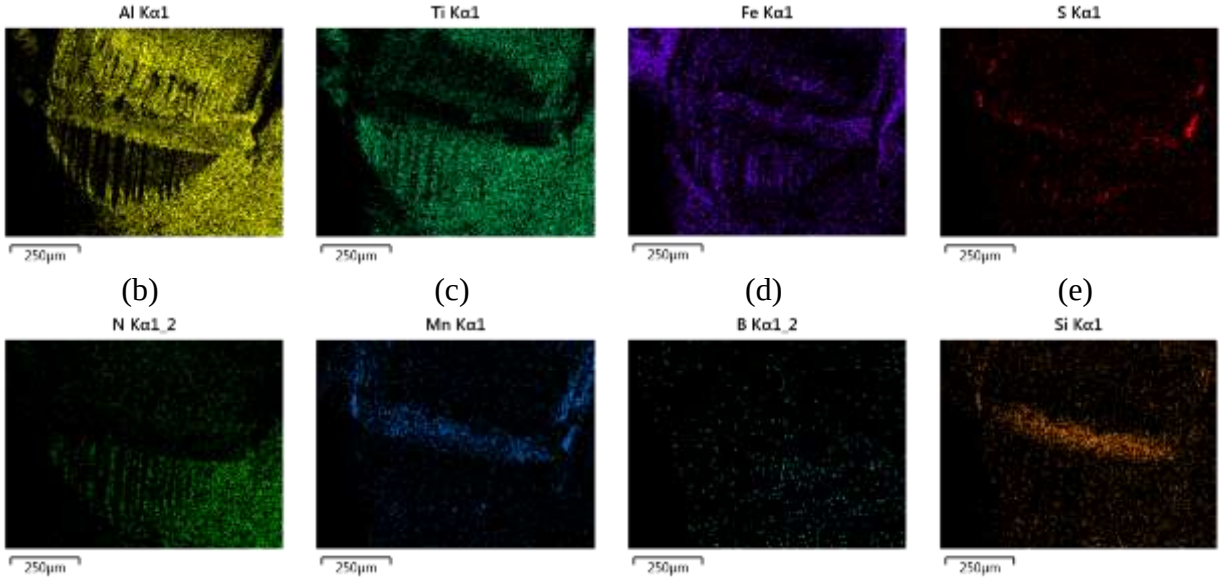

Figure 5.31 CU3 Wear inspection and EDS analysis performed in SEM: (a) BEC image and the distribution of (a)Ti, (b)Al, (c)Ti, (d)Fe, (e)S, (f)N, (g)Mn, (h)B, and (i)Si element.

5.4.4 Summary of MMRI coating

1. CVD coating Al2O3 (15-micron thickness) performed slightly better than TiAlN (5-micron thickness) in terms of tool life performance. Figure 5.26 shows that using the same substrate, the Al2O3 CVD coating improved tool life by 1279% (from 960m to 12283.8m) and the TiAlN PVD MMRI coating improved tool life by 1053% (from 960m to 10111.5m).

2. For U3, both TiAlN and TiCN coating performed similarly in terms of tool life and wear trend. TiAlN was PVD coated, and TiCN was commercially three-layered coating. In Figure 5.27, both the TiCN multilayered PVD coating (C3) and the TiAlN PVD MMRI coating (CU3) showed a decrease in tool life compared to the uncoated U3 tool. The coating for both worn tooltips remained intact at the wear location (agree with Study B). Further investigation on U3 and coated U3 could be done at different cutting speeds (higher cutting speed).

6 Conclusions and Future direction

6.1 Conclusions

This thesis provides an overview of current state of the art low-carbon steel HSDM using different type of CBN tools. A similar tool life could be achieved if the CVD coating was substituted with a PVD coating. Under dry machining, this could achieve better productivity and finish than the regular HSM process.

Uncoated CBN tools:

1. The dominant wear mode in the uncoated CBN tool (with an AISI 1018 workpiece) was abrasion. Oxidation also occurred during the early stage of machining. EDS detection of Fe particles revealed that the main wear mechanism on the flank face is soft adhesion of CBN particles, which leave abrasion marks on the flank face of the tool [40].

2. In uncoated CBN tools, abrasion resistance improved with lower CBN content, finer grain size and better binder material (TiCN performed better than TiN and WCo binders). At high cutting speeds, the binder material was easily softened, significantly reducing tool life due to the high temperature.

Coated CBN tools:

3. Al2O3 and TiAlN coatings improved CBN tool life (TiN binder) and are therefore recommended for LCS machining. According to Naskar and Chattopadhyay, these coatings not only feature good performance in CBN tools with LCS, but also carbide tools with C20 (low carbon content steel) during the finishing process [4].

4. CVD Al2O3 thick coating performed slightly better than PVD TiAlN. AlTiN and TiCN coated CBN tools did not provide significant tool life improvement. According to Naskar and Chattopadhyay's study, the TiCN coating has a greater solubility in steel than the TiAlN or Al2O3 coating. Due to TiCN coating's higher rate of dissolution and due to the low carbon percentage of C20 (AISI1018 shares the similar properties) the diffusion gradient will be higher and the wider interstitial space will enhance the solubility of coating material into steel, which is the reason for the TiCN coatings' higher flank wear rate [4].

5. The TiAlN coating applied in the MMRI institute showed a tool life improvement compared to a CVD Al2O3 and a TiCN multi-layer coating. The thickness of the TiAlN coating is 5 µm, which is lower than that of the C1 commercial coated tool with a 15 µm thick CVD applied Al2O3 coating. At the same time, the performance of the two coatings is similar. This shows that the MMRI coated tool provides better performance at a lower cost (CVD compare to PVD requires higher deposition temperature and time, which consumes more time and energy during the process [36])

6. The best performance in this thesis study was delivered by an uncoated CBN tool with a TiCN binder, grain size of 1 micron and 40% to 45% CBN content. The end-of-tool-life study also showed abrasion wear only on the coating, no coating delamination and no substrate material exposure for C2, C3, and C4. This demonstrates that the chemical interaction of the binder material might interrupted by the applied coating. C3 and CU3 coated tools were the best performers of the selected coated tools with a good supporting substrate. TiCN proved to be a relatively better binder material, which can protect the embedded CBN particles from being worn away during the machining, thus prolonging the tool life.

Future Work

The tribological behaviour of the uncoated CBN tool with TiCN binder material can be further studied in the future to evaluate the effect of the binder material, and what happened during the HSDM process to elongate the tool life. More experiments at different cutting speeds for the same cutting tool and coating combinations could be carried out. In addition, more techniques could be used to investigate this such as FEA. TiCN binder material performed best in this study, yet other binder materials may be discovered that outperform it. One potential example is TiC binder according to Aizawa et al. [55]. Future studies should involve material properties such as residual stress, coating adhesion and possible chemical reactions at the workpiece-tool interface. These properties should provide an overview of the tribological process in the TiCN uncoated CBN tool with LCS during HSDM.

Reference

[1] Y. Ding and S. Y. Hong, “Improvement of Chip Breaking in Machining Low Carbon Steel by Cryogenically Precooling the Workpiece,” *J. Manuf. Sci. Eng.*, vol. 120, no. 1, p. 76, 1998.

[2] B. Selçuk, R. Ipek, M. B. Karamiş, and V. Kuzucu, “An investigation on surface properties of treated low carbon and alloyed steels (bonding and carburizing),” *J. Mater. Process. Technol.*, vol. 103, no. 2, pp. 310–317, 2000.

[3] H. Schulz and T. Moriwaki, “High-speed Machining,” *CIRP Ann. - Manuf. Technol.*, vol. 41, no. 2, pp. 637–643, 1992.

[4] A. Naskar and A. K. Chattopadhyay, “Investigation on flank wear mechanism of CVD and PVD hard coatings in high speed dry turning of low and high carbon steel,” *Wear*, vol. 396–397, pp. 98–106, 2018.

[5] K. S. Neo, M. Rahman, X. P. Li, H. H. Khoo, M. Sawa, and Y. Maeda, “Performance evaluation of pure CBN tools for machining of steel,” *J. Mater. Process. Technol.*, vol. 140, no. 1-3 SPEC., pp. 326–331, 2003.

[6] G. S. Goindi and P. Sarkar, “Dry machining: A step towards sustainable machining – Challenges and future directions,” *J. Clean. Prod.*, vol. 165, pp. 1557–1571, 2017.

[7] Y. Liu, “Influence of Free Ferrite Content on the Machinability of GCI using CBN tool,” *MacSphere*, vol. 91, pp. 399–404, 2018.

[8] M. T. Edward and P. K. Wright, *Metal Cutting*, Four. Elsevier, 2000.

[9] C. M. Rao and K. Venkatasubbaiah, “Optimization of Surface Roughness in CNC Turning

Using Taguchi Method and ANOVA," *Int. J. Adv. Sci. Technol.*, vol. 93, no. 1, pp. 1–14, 2016.

[10] S. Dhiman, R. Sehgal, S. K. Sharma, and V. S. Sharma, "Machining behavior of AlSI 1018 steel during turning," *J. Sci. Ind. Res. (India).*, vol. 67, no. 5, pp. 355–360, 2008.

[11] S. Chinchanikar and S. K. Choudhury, "Machining of hardened steel - Experimental investigations, performance modeling and cooling techniques: A review," *Int. J. Mach. Tools Manuf.*, vol. 89, pp. 95–109, 2015.

[12] R. A. Grange, "Estimating the hardenability of carbon steels," *Metall. Trans.*, vol. 4, no. 10, pp. 2231–2244, 1973.

[13] Y. Ozcatalbas and F. Ercan, "The effects of heat treatment on the machinability of mild steels," *J. Mater. Process. Technol.*, vol. 136, no. 1–3, pp. 227–238, 2003.

[14] SANDVIK, "SANDVIK Materials," *SANDVIK Coromant*, vol. 37, 2010.

[15] M. I. Group, "Tungaloy Catalogue 2018/2019," *Tungaloy Gen. Cat.*, vol. 1348, 2018.

[16] Sumitomo, "Sumitomo CBN," *Sumitomo*, 2019. [Online]. Available: https://www.sumitomotool.com/fileadmin/user_upload/Blaetterkataloge/catalogs/Sumitomo_Catalogue_2018-2019_L-M/pdf/complete_print.pdf. [Accessed: 02-Jul-2019].

[17] P. Fallböhmer, C. A. Rodríguez, T. Özel, and T. Altan, "High-speed machining of cast iron and alloy steels for die and mold manufacturing," *J. Mater. Process. Technol.*, vol. 98, no. 1, pp. 104–115, 2000.

[18] P. S. Sreejith and B. K. A. Ngoi, "Dry machining: Machining of the future," *J. Mater. Process. Technol.*, vol. 101, no. 1, pp. 287–291, 2000.

[19] M. Dogra, V. S. Sharma, A. Sachdeva, N. M. Suri, and J. S. Dureja, “Tool wear, chip formation and workpiece surface issues in CBN hard turning: A review,” *Int. J. Precis. Eng. Manuf.*, vol. 11, no. 2, pp. 341–358, 2010.

[20] R. Mustafizur, W. Zhi-Gang, and W. Yoke-San, “A review on High-Speed Machining of Titanium Alloys,” *Rev. Adv. Mater. Sci.*, vol. 36, no. 2, pp. 89–111, 2006.

[21] KENNAMETAL, “Master Catalogue 2018 Turning Tools,” vol. 37, pp. 302–337, 2018.

[22] H. CNC, “Cutting Insert ISO,” 2018. [Online]. Available: http://www.helmancnc.com/general-turning-insert-nomenclature-for-cnc-dummies/. [Accessed: 03-Jul-2019].

[23] Nikko, “Nikko Tools,” *SORMA Tools*, 2019. [Online]. Available: https://www.nikkotools.com/catalogue/Update2019/Nikko_Tools_Update2019.html#p=5. [Accessed: 03-Jul-2019].

[24] J. G. Corrêa, R. B. Schroeter, and Á. R. Machado, “Tool life and wear mechanism analysis of carbide tools used in the machining of martensitic and supermartensitic stainless steels,” *Tribol. Int.*, vol. 105, no. July 2016, pp. 102–117, 2017.

[25] G. K. Dosbaeva, M. A. El Hakim, M. A. Shalaby, J. E. Krzanowski, and S. C. Veldhuis, “Cutting temperature effect on PCBN and CVD coated carbide tools in hard turning of D2 tool steel,” *Int. J. Refract. Met. Hard Mater.*, vol. 50, pp. 1–8, 2015.

[26] S. Debnath, M. M. Reddy, and Q. S. Yi, “Influence of cutting fluid conditions and cutting parameters on surface roughness and tool wear in turning process using Taguchi method,” *Meas. J. Int. Meas. Confed.*, vol. 78, pp. 111–119, 2016.

[27] M. M. A. Khan, M. A. H. Mithu, and N. R. Dhar, “Effects of minimum quantity lubrication

on turning AISI 9310 alloy steel using vegetable oil-based cutting fluid," *J. Mater. Process. Technol.*, vol. 209, no. 15–16, pp. 5573–5583, 2009.

[28] Y. Sahin and A. R. Motorcu, "Surface roughness model for machining mild steel with coated carbide tool," *Mater. Des.*, vol. 26, no. 4, pp. 321–326, 2005.

[29] K. Weinert, "Einsatz moderner Schneidstoffe in der Zerspanung.," *Kolaska*, vol. 71–95, 2003.

[30] E. Bassett, J. Köhler, and B. Denkena, "On the honed cutting edge and its side effects during orthogonal turning operations of AISI1045 with coated WC-Co inserts," *CIRP J. Manuf. Sci. Technol.*, vol. 5, no. 2, pp. 108–126, 2012.

[31] T. Mori and S. Nojiri, "Topological gravity motivated by renormalization group," *Symmetry (Basel).*, vol. 10, no. 9, pp. 100–110, 2018.

[32] Y. Sahin, "Comparison of tool life between ceramic and cubic boron nitride (CBN) cutting tools when machining hardened steels," *J. Mater. Process. Technol.*, vol. 209, no. 7, pp. 3478–3489, 2009.

[33] Y. K. Chou, C. J. Evans, and M. M. Barash, "Experimental investigation on CBN turning of hardened AISI 52100 steel," *J. Mater. Process. Technol.*, vol. 124, no. 3, pp. 274–283, 2002.

[34] Z. N. Farhat, "Wear mechanism of CBN cutting tool during high-speed machining of mold steel," *Mater. Sci. Eng. A*, vol. 361, no. 1–2, pp. 100–110, 2003.

[35] Z. C. Lin and D. Y. Chen, "A study of cutting with a CBN tool," *J. Mater. Process. Tech.*, vol. 49, no. 1–2, pp. 149–164, 1995.

[36] K. D. Bouzakis, N. Michailidis, G. Skordaris, E. Bouzakis, D. Biermann, and R. M'Saoubi,

"Cutting with coated tools: Coating technologies, characterization methods and performance optimization," *CIRP Ann. - Manuf. Technol.*, vol. 61, no. 2, pp. 703–723, 2012.

[37] Y. K. Chou and C. J. Evans, "Cubic boron nitride tool wear in interrupted hard cutting," *Wear*, vol. 225–229, no. I, pp. 234–245, 1999.

[38] A. Wyczesany, E. Benko, J. Skrzypek, B. Kro, and T. L. Barr, "cBN – TiN , cBN – TiC composites : chemical equilibria , microstructure and hardness mechanical investigations," vol. 8, pp. 1838–1846, 1999.

[39] A. Mckie, J. Winzer, I. Sigalas, and M. Herrmann, "Mechanical properties of cBN – Al composite materials," vol. 37, pp. 1–8, 2011.

[40] Y. Huang, Y. K. Chou, and S. Y. Liang, "CBN tool wear in hard turning: A survey on research progresses," *Int. J. Adv. Manuf. Technol.*, vol. 35, no. 5–6, pp. 443–453, 2007.

[41] A. J. de Oliveira, D. Boing, and R. B. Schroeter, "Effect of PCBN tool grade and cutting type on hard turning of high-chromium white cast iron," *Int. J. Adv. Manuf. Technol.*, vol. 82, no. 5–8, pp. 797–807, 2016.

[42] S. Thamizhmanii and S. Hasan, "Performance of CBN and PCBN Tools on the Machining of Hard AISI 440C Martensitic Stainless Steel," *Adv. Mater. Res.*, vol. 264–265, no. 201 1, pp. 1137–1147, 2011.

[43] M. Narasimha, R. R. Kumar, and A. Kassie, "Performance of Coated Carbide Tools," *Int. J. Eng. Sci.*, vol. 2, no. 6, pp. 47–54, 2013.

[44] Organization International Standard, "Tool-life testing with single-point turning tools ISO 3685 2nd," 1993.

[45] S. Y. Luo, Y. S. Liao, and Y. Y. Tsai, "Wear characteristics in turning high hardness alloy

steel by ceramic and CBN tools," *J. Mater. Process. Technol.*, vol. 88, no. 1, pp. 114–121, 1999.

[46] J. P. Costes, Y. Guillet, G. Poulachon, and M. Dessoly, "Tool-life and wear mechanisms of CBN tools in machining of Inconel 718," *Int. J. Mach. Tools Manuf.*, vol. 47, no. 7–8, pp. 1081–1087, 2007.

[47] F. Klocke, *Manufacturing processes 1: turning, milling, drilling, no. 7858*. Springer, 2011.

[48] S. Hogmark, S. Jacobson, and M. Larsson, "Design and evaluation of tribological coatings," *Wear*, vol. 246, no. 1–2, pp. 20–33, 2000.

[49] M. Chowdhury, "WEAR BEHAVIOUR OF COATED CARBIDE TOOLS DURING MACHINING OF Ti6Al4V AEROSPACE ALLOY," 2016.

[50] L. Ning, "Nano-multilayered Self-adaptive Hard PVD Coatings for Dry High Performance Machining," p. 218, 2007.

[51] H. A. J. U, "Multicomponent and multiphase hard coatings for tribological applications," *Surf. Coatings Technol.*, pp. 433–440, 2000.

[52] C. E. H. Ventura, J. Köhler, and B. Denkena, "Influence of cutting edge geometry on tool wear performance in interrupted hard turning," *J. Manuf. Process.*, vol. 19, pp. 129–134, 2015.

[53] G. S. Fox-Rabinovich and A. I. Kovalev, *Self-Organization and Structural Adaptation during Cutting and Stamping Operations*. Boca Raton, NW, USA: CRC Press, 2006.

[54] G. Fox-Rabinovich, I. Gershman, M. Hakim, M. Shalaby, J. Krzanowski, and S. Veldhuis, "Tribofilm Formation As a Result of Complex Interaction at the Tool/Chip Interface during Cutting," *Lubricants*, vol. 2, no. 3, pp. 113–123, 2014.

[55] T. Aizawa, A. Mitsuo, S. Yamamoto, T. Sumitomo, and S. Muraishi, “Self-lubrication mechanism via the in situ formed lubricious oxide tribofilm,” *Wear*, vol. 259, no. 1–6, pp. 708–718, 2005.

[56] AZoM, “AZO Materials AISI 1018.” [Online]. Available: https://www.azom.com/article.aspx?ArticleID=6115. [Accessed: 24-Jun-2019].

[57] Kennametal, “KC730,” *Kennametal*, 2019. [Online]. Available: https://cets.com/resources/kennametal-grades. [Accessed: 03-Jul-2019].

[58] Kennametal, “KB1340,” *Kennametal*, 2019. [Online]. Available: https://www.kennametal.com/en/products/20478624/47535256/63745063/63745065/100147804/100147805/100000561.html?orderNumber=3764792. [Accessed: 02-Jul-2019].